

OCEAN DRILLING PROGRAM
LEG 112 PRELIMINARY REPORT
PERU CONTINENTAL MARGIN

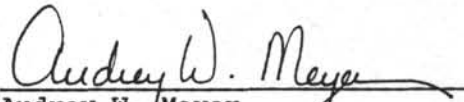
Roland von Huene
Co-Chief Scientist, Leg 112
U.S. Geological Survey MS 999
345 Middlefield Road
Menlo Park, CA 94025

Erwin Suess
Co-Chief Scientist, Leg 112
College of Oceanography
Oregon State University
Corvallis, OR 97331

Kay-Christian Emeis
Staff Scientist, Leg 112
Ocean Drilling Program
Texas A&M University
College Station, TX 77843-3469



Philip D. Rabinowitz
Director
ODP/TAMU



Audrey W. Meyer
Manager of Science Operations
ODP/TAMU



Louis E. Garrison
Deputy Director
ODP/TAMU

February 1987

This informal report was prepared from the shipboard files by the scientists who participated in the cruise. The report was assembled under time constraints and is not considered to be a formal publication which incorporates final works or conclusions of the participating scientists. The material contained herein is privileged proprietary information and cannot be used for publication or quotation.

Preliminary Report No. 12

First Printing 1987

Copies of this publication may be obtained from the Director, Ocean Drilling Program, Texas A&M University, College Station, Texas 77843-3469. In some cases, orders for copies may require a payment for postage and handling.

D I S C L A I M E R

This publication was prepared by the Ocean Drilling Program, Texas A&M University, as an account of work performed under the international Ocean Drilling Program which is managed by Joint Oceanographic Institutions, Inc., under contract with the National Science Foundation. Funding for the program is provided by the following agencies:

Department of Energy, Mines and Resources (Canada)

Deutsche Forschungsgemeinschaft (Federal Republic of Germany)

Institut Francais de Recherche pour l'Exploitation de la Mer (France)

Ocean Research Institute of the University of Tokyo (Japan)

National Science Foundation (United States)

Natural Environment Research Council (United Kingdom)

European Science Foundation Consortium for the Ocean Drilling Program
(Belgium, Denmark, Finland, Iceland, Italy, Greece, the Netherlands,
Norway, Spain, Sweden, Switzerland, and Turkey)

Any opinions, findings and conclusions or recommendations expressed in this publication are those of the author(s) and do not necessarily reflect the views of the National Science Foundation, the participating agencies, Joint Oceanographic Institutions, Inc., Texas A&M University, or Texas A&M Research Foundation.

SCIENTIFIC REPORT

The scientific party aboard JOIDES Resolution for Leg 112 of the Ocean Drilling Program consisted of:

Erwin Suess, Co-Chief Scientist (Oregon State University, Corvallis, OR)
Roland von Huene, Co-Chief Scientist (U. S. Geological Survey, Menlo Park, CA)
Kay-Christian Emeis, Staff Scientist (Ocean Drilling Program, Texas A&M University, College Station, TX)
Jacques Bourgois (Universite Pierre et Marie Curie, Paris, France)
Jose del C. Cruzado (Petroleos del Peru, Lima, Peru)
Patrick De Wever (Universite Pierre et Marie Curie, Paris, France)
Geoffrey Eglinton (University of Bristol, Bristol, England)
Robert Garrison (University of California, Santa Cruz, Santa Cruz, CA)
Matt Greenberg (Lamont-Doherty Geological Observatory, Palisades, NY)
Elard Herrera (Petroleos del Peru, Lima, Peru)
Phil Hill (Bedford Institute of Oceanography, Nova Scotia, Canada)
Masako Ibaraki (Shizuoka University, Shizuoka, Japan)
Miriam Kastner (Scripps Institution of Oceanography, La Jolla, CA)
Alan E. S. Kemp (The University, Southampton, England)
Keith Kvenvolden (U. S. Geological Survey, Menlo Park, CA)
Robert Langridge (Queen's University, Ontario, Canada)
Nancy Lindsley-Griffin (University of Nebraska, Lincoln, NE)
Robert McCabe (Texas A&M University, College Station, TX)
Janice Marsters (Bedford Institute of Oceanography, Nova Scotia, Canada)
Erlend Martini (Geologisch-Palaeontologisches Institut der Universitaet, Frankfurt, FRG)
Leonidas Ocola (Instituto Geofisico del Peru, Lima, Peru)
Johanna Resig (University of Hawaii, Honolulu, HI)
Agapito Wildredo Sanchez (Instituto Geologico Minero y Metalurgico, Lima, Peru)
Hans Schrader (Oregon State University, Corvallis, OR)
Todd M. Thornburg (Oregon State University, Corvallis, OR)
Gerold Wefer (Universitaet Bremen, Bremen, FRG)
Makoto Yamano (University of Tokyo, Tokyo, Japan)

INTRODUCTION

Leg 112 set out to investigate the tectonic and oceanographic history recorded in the sediment sequence of the forearc basins (Salaverry, Lima, Pisco, Yaquina, and Trujillo basins; Figure 1) and the adjacent continental slope of the convergent margin off Peru. Objectives included determining vertical tectonic movement in the basins and on the continental margin, and assessing the timing and the spatial extent of these movements. By integrating tectonic events of the margin and the continent a better understanding of tectonic mechanisms of convergent margins could be obtained. The paleoceanographic objectives addressed the history of coastal upwelling along the Peruvian margin specifically since Miocene time, when the present Pacific Ocean circulation pattern was established. In addition, the Pleistocene sedimentary sequence was examined for signals of a climatic record with a very high temporal resolution. Accumulation and flux rates for biological and clastic components were to be estimated for the Peru upwelling system, one of the most prominent and most continuous sinks of nutrients of the world's ocean. These estimates will be employed to fine-tune global mass-balance calculations. Diagenesis in the organic carbon-rich upwelling facies leads to chemical conditions favorable for the precipitation of a carbonate, sulfide, and phosphorite mineral assemblage of distinct chemistry and isotopic composition. Conditions of formation of these diagenetic products were another major paleoenvironmental objective. The upwelling characteristics established for the sediments off Peru will eventually be used to diagnose ambiguous ancient upwelling facies in other parts of the world and from different geologic periods.

In brief, the pre-cruise Leg 112 objectives were intended:

- To reconstruct the uplift and subsidence history of the forearc area and relate these vertical movements to tectonic accretion and the erosion of older strata at the Pacific margin of the South American craton.
- To study the nature and age of the transition zone that lies between the lower-slope accretionary complex and the metamorphic block of continental affinity.
- To investigate the age of the metamorphic basement underlying the outer Andean margin, as well as pressure and temperature conditions of metamorphism through time.
- To document vertical movement of the continental margin as a response to subduction of the Nazca Plate under the continental block of South America.
- To reconstruct the paleoceanographic conditions of the upper-slope basin deposits in terms of the response of the biological and sedimentary system to fluctuations in intensity and source of upwelling waters.
- To quantify biogenic and clastic fluxes for an evaluation of interactions between sea level, climate, and oceanic circulation.
- To understand the conditions that lead to the formation of dolomites, phosphorites, and cherts in these upper-slope basin deposits.
- To show that microbial activity persists to considerable depths and contributes greatly to the diagenetic environment in organic carbon-rich sediments.

JOIDES Resolution departed Callao, Peru, on October 30, 1986. During

the 51 days of operations, 27 holes were drilled at 10 sites to meet the scientific objectives mentioned above. A total of 6,754 m of sediment were penetrated of which 4,701.3 m were cored and 2,578 m were recovered (Table 1). The ship returned to Callao on December 19.

DRILLING RESULTS

The following site-by-site reports summarize the major results obtained and give the conclusions reached for each drill site. The sequence is in chronological order. A synthesis of the major drilling results of Leg 112 with regard to tectonic and paleoceanographic objectives follows these site-by-site reports (see pages 15-30).

SITE 679 (450 m water depth)

Site 679 was positioned on the outer continental shelf of Peru (Table 1; Figure 1) to sample the distal edge of the sediment lens beneath a modern upwelling plume and continue into the underlying sediment section to sample ancient sediment of a similar origin but at different stages of diagenesis. In addition, the stratigraphic column was to be sampled to the crystalline basement that extends offshore across the continental shelf and along the upper part of the landward slope of the Peru Trench. From that stratigraphic column, which is here one-third of its thickness downslope, the vertical tectonic motion of the shelf during the Andean orogeny might be established. This site is the landward point on a transect of sites (679, 682, 688) targeted to investigate the vertical tectonic history of the continental margin.

The 5 holes drilled at this site are in a water depth of about 450 m and the deepest penetration was to 359.3 mbsf (Table 1). Hole 679E was terminated about 100 m above crystalline basement for reasons of safety. Five lithostratigraphic units were recognized. The first three units were separated on the basis of diatom and carbonate content. The last two units are principally mudstone and siltstone. Although many hiatuses are suspected, they are difficult to recognize except where marked by conglomerates of phosphate nodules or by winnowed horizons. Lithostratigraphic Unit 1 (0-45 mbsf) consists of olive to dark-gray diatom-foraminifer mud. A hiatus may separate this unit from Unit 2 (45-101 mbsf), which consists of olive to black diatomaceous mud with numerous microfaults and fluid-escape structures. The first two lithostratigraphic units were deposited under hemipelagic conditions in the Pliocene and Pleistocene and were subject to periodic bottom currents. Unit 3 of late Miocene age (101-245 mbsf) consists of olive gray to very dark gray diatomaceous mud, silt, and fine sand. A sequence of well-preserved primary structures shows evidence of clastic traction transport and possibly storm events. Lithostratigraphic Unit 4 of middle Miocene age (245-338 mbsf), separated from Unit 3 by an unconformity, consists of light gray to dark gray mudstone and siltstone with periodic calcite cementation and numerous thin turbidite structures. A hiatus separates lithostratigraphic Unit 4 from Unit 5 (338-359 mbsf) which consists of very dark gray shale deposited in an anoxic pelagic and hemipelagic environment in the middle Miocene.

The Site 679 biostratigraphy was based on abundant siliceous

microfossils and sporadic calcareous microfossils. Each of the intervals is separated by a major hiatus. Planktonic foraminifer and diatom assemblages indicate temperate surface-water temperatures similar to those found today along the Peruvian coastal upwelling areas. Benthic foraminifers occur in assemblages of an in-situ and a transported character. All in-situ assemblages lived in upper bathyal water depths and are most common in the upper two lithostratigraphic units. Assemblages transported from shallower depths are most common in the lower lithostratigraphic units. There are no indications of significant vertical tectonic movement since about 12 Ma.

The sediment section reveals considerable early diagenesis, in particular, the early formation of carbonate-F-apatite (francolite), dolomite, pyrite, and, to a lesser extent, of opal-CT chert. These constituents have formed layers and nodules or are disseminated within the sediments. Preliminary examination of the distribution of carbonate, phosphate, and opal-A revealed a clear progression of dolomite formation downhole; dolomite occurrences range from disseminated rhombs, thin layers, and small nodules in the upper units to more massive beds and larger nodules in the deeper units. Cementation by calcite was first observed in lithostratigraphic Unit 3. Numerous layers composed exclusively of diatom tests seem to enhance early diagenetic processes, perhaps by providing increased permeability and porosity for chemical reactants.

The interstitial-water chemistry at Site 679 is dominated by bacterial degradation of organic matter, mainly in the sulfate-reduction zone, and consequently by increased concentrations of H_2S , phosphate, ammonia, and pronounced higher alkalinity. These dissolved components control the diagenetic formation of francolite, dolomite, calcite, and pyrite. Superimposed on this distribution pattern of dissolved species is a freshwater incursion in lithostratigraphic Unit 4. In this zone, chloride decreases from the seawater value of 559 mmol/L, the observed value in the upper 172 m, to a minimum value of 345 mmol/L (63% of seawater). The freshwater incursion may be related to either ancient or recent flow from aquifers in the Andes or the presence of a fossil freshwater lens.

At Site 679, the compressed stratigraphic section contains a record of late Neogene and Quaternary coastal upwelling. The relatively sparse clastic influx compared to the rate at which the organic carbon-rich upwelling products accumulate produces a chemical environment conducive to the rapid formation of dolomites, phosphates, and sulfides during the early stages of diagenesis. The resulting anoxic bottom environment and the absence of bioturbation allow primary sedimentary structures characteristic of the pelagic and hemipelagic environment to be preserved. Also preserved are subsequently formed fluid-escape structures and microfaults related to the extensional and shear deformation associated with downslope gravity movement. Under this section dominated by upwelling facies is another facies dominated by turbidites with terrigenous and nearshore affinities of middle Miocene age. This latter facies contains pore fluids significantly diluted by freshwater, which have migrated from another environment.

SITE 680 (250 m water depth)

Site 680 is centered on an E-W transect of three sites (679, 680, 681) across a lens-shaped sedimentary body of coastal upwelling deposits of the

Peruvian outer shelf and upper slope (Table 1; Figure 1). Coring at Site 680 sampled an expanded record, as compared to Site 679, of late Pleistocene to Holocene coastal upwelling. The sediment record at this site documents the vertical and lateral shifts of the oxygen-minimum layer, organic-carbon preservation, and flux rates of sediment constituents through time in response to sealevel fluctuations. In the lower section, below the continuous reflector at 56.4 mbsf, a lower Pliocene to Pleistocene sequence was sampled which has more terrigenous affinities, a sequence which was previously encountered at Site 679.

Three holes were drilled at Site 680. Three lithostratigraphic units were distinguished. Unit 1 (0-48 mbsf) is a thinly laminated dark olive green foraminifer-diatomaceous mud recognized in Hole 680A. It was deposited during the late Pleistocene and Holocene and is rich in organic matter (6 to 10%). The Matuyama/Brunhes boundary was identified near the base of this unit, at 36 mbsf. Lithostratigraphic Unit 2 (48-56.4 mbsf) consists of thinly laminated diatomaceous silty mud with authigenic dolomites and phosphates concentrated in diatom-rich laminae or sandy layers. Unit 2 is in sharp contact with Unit 3 at 56.4 mbsf. Lithostratigraphic Unit 3 contains substantial amounts of clastic material associated with several beds of phosphatic conglomerates. All lithologic units contain well-preserved and abundant diatom floras, but appear to be repeatedly broken by hiatuses. In Hole 680B the same upper Quaternary sequence was piston-cored with excellent recovery to a depth of 92 mbsf; core recovery was poor during subsequent extended core barrel (XCB) drilling through lower Pliocene sediments to the bottom of Hole 680B at 195.5 mbsf. Feldspathic clastic sediments associated with beds of phosphatic conglomerates and sands are characteristic lithologies of this Pliocene sequence. Four advanced piston core (APC) cores (0-34 mbsf) were cored in Hole 680C, with 100% recovery, before the hole was terminated due to a sand-line failure. Samples from this hole were preserved for shorebased microbiological, organic geochemical, and geotechnical studies.

At Site 680 all stages of dolomite, calcite, and phosphate formation and replacement are common. Dolomite is the predominant authigenic phase and was found as disseminated rhombs at only 0.8 mbsf. Phosphates occur in all units as thinly laminated beds of friable carbonate-fluorapatite, concentrated in diatom-rich laminae, and as dark, dense peloids and nodules typically in sandy and conglomeratic strata. This sediment sequence and its pore water and dissolved gas chemistries reveal considerable early diagenetic activity which is affected by highly saline pore fluids discovered at this site. Salinities, chloride, and other dissolved major ion contents in pore waters increased to about twice the concentrations of normal seawater at 195.5 mbsf, suggesting incursion of hypersaline fluid.

Despite the preliminary nature of shipboard studies, the cores from Site 680 contain all components of a well-developed upwelling facies and reveal unique low-temperature diagenetic reactions sustained by an incursion of brine. Models of diagenesis in Peruvian upwelling sediments must account for the effects of interchange between such hypersaline solutions and primary constituents of upwelling sediment.

SITE 681 (150 m water depth)

Site 681 is the shallowest and most landward target along the E-W transect crossing the upwelling deposits of the Peruvian shelf and upper slope (Table 1; Figure 1). Of the three sites (679, 680, and 681) along the transect, Site 681 is located closest to the origin of coastal upwelling centers around the headlands near 11°S. The water depth of 150.5 m nearly coincides with the top of the oxygen-minimum zone. Because of the high sedimentation rates at Site 681, an expanded Quaternary sediment record was obtained for studies of temporal changes in the main upwelling parameters, i.e., salinity, temperature, nutrient composition. At this site, interest focused specifically on the effect of fluctuations in the upper boundary of the oxygen-minimum zone impinging on the shelf.

The base of the most recent upwelling deposits is at approximately 130 mbsf according to the seismic records, indicating that here the thickness of the upper Pleistocene and Holocene sequence is about twice that encountered at Site 680. Four lithostratigraphic units were recognized at Site 681. Units 1 and 3 (0 to 35 mbsf and 96 to 135 mbsf, respectively) consist of repeated sequences of dark olive gray diatomaceous mud with laminae of diatom ooze. Unit 2 (35 to 96 mbsf) is an interval of massive dark gray terrigenous muds with some degree of bioturbation. Magnetic reversals (?Blake event at 18 mbsf; the Matuyama/Brunhes paleomagnetic boundary at 83 mbsf) and numerous floral markers facilitate cross correlation between individual holes. Within these units there is evidence for relative sea-level fluctuations and cyclic sedimentation based on the presence of erosion surfaces, phosphatic lag deposits, and repeated intervals of increased influx of terrigenous clastics.

Well-preserved and abundant diatom floras characteristic of "oceanic" and "upwelling" conditions alternate within lithostratigraphic Units 1 and 3. Unit 3 contains more heavily silicified diatom assemblages, indicating deposition during glacial periods. The same climatic trends are indicated by the benthic and planktonic foraminiferal assemblages containing well-known upwelling species.

In lithostratigraphic Unit 4, below 135.3 mbsf to the bottom of Hole 681A at 187.0 mbsf, dark gray silty sand with sparse intervals of diatomaceous mud, with some scattered cemented dolomite nodules, was sampled. Unit 4 appears similar to the lithofacies encountered at Sites 679 and 680, represented by the continuous reflective sequence of Pliocene strata.

At Hole 681C, 86.4 m of core was recovered and the materials frozen to complete sampling for geomicrobiology, organic geochemistry, and physical properties projects which had been cut short at the previous site.

At Site 681 the sediment, its pore water, and dissolved gas chemistries revealed extensive early diagenetic processes. Throughout the section, organic matter is mineralized by microbial sulfate reduction. Authigenic dolomite, found as rhombs, nodular, and blocky zones and thinly bedded layers, is one product of diagenesis within the upwelling facies. Another product is phosphorites. Early diagenetic reactions are affected by highly saline pore fluids similar to those discovered at the previous site.

Chloride and other dissolved major ion contents increase to concentrations twice those of seawater near the bottom of Hole 681B.

The preliminary shipboard studies of Site 681 sediments indicate that the section records changes in the position and intensity of the coastal upwelling regime. This oceanographic process is reflected in well-preserved and abundant diatom floras that occur in laminated muds alternating with bioturbated silty muds. Synchronous alternations in the amount and type of organic matter appear similar in frequency to those of major glacial/interglacial cycles. The large amplitudes of Pleistocene sea-level fluctuations have not erased the upwelling record at Site 681 because tectonic subsidence during deposition maintained optimal water depth for its preservation.

SITE 682 (3788 m water depth)

The litho- and biostratigraphy of the 437 m penetrated is divided into four lithostratigraphic units. Unit 1 extends from 0 to 114 mbsf and records a typical hemipelagic continental-slope environment consisting of mud and biogenic components derived from the coastal upwelling regime upslope. The Pliocene and Pleistocene sediments are poorly laminated diatomaceous mud mixed with terrigenous sand and interbeds of foraminifer- and nannofossil-bearing diatomaceous mud. Toward the bottom of the interval the terrigenous components increase. The sediments contain all the diagenetic products associated with upwelling sediment that were noted in previous Leg 112 sites except phosphorites. The benthic foraminiferal assemblages lived at the present water depths, and rare reworked microfossils were recovered. The boundary between lithostratigraphic Units 1 and 2 coincides with the boundary between Pliocene and upper middle to upper Miocene sediments.

Unit 2 (114 to 311 mbsf) consists of diatomaceous mudstones which are more consolidated, fracture readily, and deform in a brittle manner. Micritic-dolomite layers and authigenic calcite crystals appear in the upper Miocene. The benthic foraminiferal assemblages lived at middle rather than lower bathyal depths. Approximately 30 m below the hiatus the sediment is composed of materials eroded upslope as seen in the displacement of lower Miocene nannofossils, benthic foraminifers, and a mixed assemblage of diatoms. A zone of poor recovery yielding only gravel marks an abrupt increase in consolidation of the sediment and signals the boundary between Units 2 and 3. Unit 3 (311 to 404 mbsf) is a section of lower Oligocene to middle Miocene mudstones which are texturally coarser, more terrigenous, and less diatomaceous than those above. Other general lithological differences include local volcanic ash and an apparent reduced rate of sedimentation resulting partly from compaction and tectonic effects. The very inhomogeneous lithologies indicate a varied environment on the continental slope. The benthic foraminiferal assemblages recovered are of middle bathyal affinities, although a single lower bathyal assemblage with Oligocene-Miocene components was observed.

A major hiatus at approximately 400 mbsf separates lithostratigraphic Units 3 and 4 (404 to 437 mbsf). Recovery across the hiatus was poor, and the rocks are highly brecciated. Rare clasts indicate proximity to continental basement, and the recovery of only gravel corresponds in

character to the high amplitude and broken reflections observed in seismic records. The middle and upper Eocene rocks below this hiatus are silty mudstones and sandstones locally cemented by authigenic carbonate. The rocks exhibit local blocky and pervasive scaly fractures as well as deformation in a semilithified state. Thus, in addition to deformation from downslope remobilization, there is also an imprint of deformation from deeper faults into shallow stratigraphic levels. Transported elements include Cretaceous nannofossils. The in-situ benthic foraminiferal assemblages indicate upper to upper-middle bathyal water depths.

Sediments recovered at Site 682 show most of the early diagenetic products that were previously seen in the upwelling sediments of the upper slope and shelf (Sites 679-681), but they also show some characteristic differences, because diagenesis is not enhanced by a hypersaline brine in the subsurface. Diagenesis leads to rapid exhaustion of interstitial sulfate at Site 682 such that methanogenesis dominates the diagenetic environment on the lower slope. Formation of gas hydrates is a consequence of the high biogenic methane contents generated here. Characteristic dissolved chloride profiles in interstitial waters signal the presence of methane hydrates, although none were observed visually. A small but significant chloride maximum around 50 mbsf is the first evidence ever recorded for the salt exclusion during gas hydrate formation. This maximum appears to advance above the gas hydrate front by diffusion. A gradual overall chloride decrease below is attributed to freshwater dilution from dissociation of gas hydrates.

SITE 683 (3071 m water depth)

A major objective at Site 683 (Table 1; Figure 1) was to establish a reference section for the upper part of the continental crust which could be compared with that for the accreted complex at the foot of the Peruvian margin. Thus the site was selected at the seaward-most area where geophysical characteristics of the continental section are observed as they are displayed at the Delfin industry drill hole, about 30 km landward. Also, at this site the water depth during the Cenozoic should have been sufficient to record fluctuations of coastal upwelling without the major hiatuses recognized in the sediment sequence on the shelf.

The Neogene lithology at Site 683 is dominated by diatomaceous mud and mudstone, which was deposited at lower bathyal depth (2 to 4 km). Because the site is presently at a depth of about 3 km, Neogene deposition has been in an upper-slope environment and is generally constant. Three lithostratigraphic units were recognized. Unit 1 (0 to 240 mbsf) consists of upper Pliocene to Pleistocene diatomaceous mud and mudstone with a calcareous-rich sequence between 30 and 67 mbsf, followed by a silt-rich sequence which grades to a poorly recovered section containing principally mud, which is characterized by numerous turbidite beds. A hiatus representing about 6.5 m.y. separates Unit 1 from the underlying lithostratigraphic Unit 2 (240 to 453 mbsf). This unconformity corresponds to seismic reflections of uniform thickness upslope to the edge of the shelf. Indication of abundant downslope transport continues deeper in the section to the unconformity at the base of the Pliocene. Unit 2 is of middle Miocene age. Lithologies consist principally of indurated diatomaceous mudstones marked by increased amounts of volcanic glass,

sparse calcareous interbeds, and rare turbidites. Some mixed microfossil assemblages still occur in this unit, but the sediments record hemipelagic sedimentation with only sparse transported clastic interbeds. The mudstones attain fissility with increasing consolidation and minor extensional microfaults.

Unit 3 (459.5 to 479 mbsf) consists of middle Eocene sediment clearly delineated in seismic records. The hiatus between the overlying Neogene and the Paleogene represents about 25 m.y.. The Eocene sediment has more sand, volcanic glass, and lithic fragments, which replace the ubiquitous diatoms of the Neogene. A well-indurated mudstone with good fissility contains some dolomicrite and micritic-limestone breccias.

In the Neogene sequence (0 to 453 mbsf), diagenesis produces many of the same products seen in samples from the shelf, but in smaller amounts. Calcite and dolomite are the main products of carbonate diagenesis. Generation of micritic-dolomite layers and authigenic calcite cements throughout the sequence follows reaction pathways controlled by organic-matter diagenesis. The gradients of dissolved chemical species are steeper than at Site 682; the maxima and minima of Ca, Mg, and alkalinity, involved in carbonate mineral diagenesis, are more pronounced. The zone of sulfate reduction is compressed toward the sediment/water interface (<20 mbsf), as is typical for rapidly accumulating organic carbon-rich sediments. Methanogenesis dominates throughout the remainder of the hole.

The organic matter at this site is primarily of marine origin. The Miocene and Pliocene sections have high organic-carbon contents (4-7 wt%) and the organic matter is immature, while the Eocene and late Pleistocene organic matter appears more mature. The decrease in chloride content with depth, and the increase in alkalinity, are similar to those obtained at previous DSDP sites where gas hydrate was visually observed. At Site 683, the upward diffusion of the residual brine from the formation of gas hydrate was observed for the first time in the anomalously high concentrations of salinity and chloride at about 100 mbsf, above the first indication of gas hydrate at 126 mbsf.

SITE 684 (426 m water depth)

Drilling at Site 684 (Table 1; Figure 1) addressed diverse objectives of coastal upwelling concerning the latitudinal variability of upwelling parameters, the facies differentiation from reworking of sediments by the poleward undercurrent, and the role of hypersaline pore fluids during early diagenesis. The variability of upwelling parameters along the Peruvian coast is expressed by the species composition of biologic assemblages, by biomarkers, and by stable isotope signals of calcareous plankton and benthos which respond to changes in water properties. Site 684 was selected to sample time intervals over which a calcareous and residual sediment facies has been accumulating on the narrow shelf characteristic of the northern Peru margin.

The site was located in a small sediment pond on the seaward flank of the Trujillo Basin in an area otherwise devoid of sediments. The pond is of limited areal extent along strike, and rests on an irregular unconformable surface separating the Miocene strata of the Trujillo Basin

from Pliocene Quaternary sediments. The continental shelf is a broad, shallow, and current-swept platform. The sediment pond lies beneath the seaward trail of numerous upwelling plumes crossing that shelf.

The sediments at Site 684 provide a record of upwelling in three distinct chronostratigraphic sections of Miocene, Pliocene, and Pleistocene age. Two hiatuses separate these sections from each other. The first hiatus occurs at 13.5 mbsf between lithostratigraphic Units 1 (0 to 13.5 mbsf) and 2 (13.5 to 17.8 mbsf) and separates well-laminated olive and gray diatomaceous muds interbedded with coarse calcareous, phosphatic, and terrigenous beds (<0.9 Ma) from underlying Pliocene bioturbated dark to olive gray mud with micro- and macrofossil-bearing sediments (3.5 to 4 Ma). Units 3 and 4 (17.8 to 38.3 mbsf and 38.3 to 54.3 mbsf, respectively) of the same sedimentary facies are separated from lithostratigraphic Unit 5 by the second hiatus that occurs at 56.2 mbsf in Hole 684A (59.5 mbsf at Hole 684C). This hiatus separates these Pliocene deposits from Miocene (older than 7 to 8 Ma) olive gray nannofossil-bearing diatomaceous mud with laminated and mottled beds which continue to the bottoms of the holes. The lithologic units and subunits which make up these three intervals alternate between hemipelagic upwelling facies and a facies which is influenced by current deposition.

The late Quaternary upwelling environment (lithostratigraphic Subunit 1A) is characterized by well-preserved floral assemblages. In the current-dominated section (Subunit 1B), normal-graded beds of shell debris, foraminifers, bone fragments, and glauconitic and phosphatic grains are common. The Pliocene depositional environment (Units 2, 3, and 4) was in shallow water and generally was less influenced by coastal upwelling. Bioturbation, erosional contacts, and coarse-grained beds are prevalent in Units 2 and 4. Diagnostic floral upwelling assemblages are rare, although organic-matter contents are quite high (7-9 wt% C-organic in Unit 3). The Miocene "upwelling" environment is characterized by numerous blooms of diatoms and coccoliths which show little evidence of reworking. They are indicative of high nutrient supply to surface waters during brief and alternating cold and warm phases. Perhaps the warm phases represent periods during which upwelling is generated from equatorial rather than Antarctic waters. Phosphoritic beds in lithostratigraphic Units 2 and 4 are condensed sequences associated with major hiatuses that correlate with eustatic lowstands of sea level. The diatomaceous units indicative of upwelling contain authigenic carbonates and friable phosphates. Calcite and dolomite are present as disseminated crystals in unlithified muds and as fully lithified nodules and beds. Intervals with pronounced concentrations of calcite and dolomite coincide with zones of significant changes in the Ca/Mg ratio of hypersaline pore waters.

These fluids were previously discovered in the subsurface of the Peru outer shelf at Sites 680 and 681, 200 km farther to the south. Microbial sulfate reduction and methanogenesis, as the important driving mechanisms of carbonate and organic matter diagenesis, are closely controlled by the brine influx. This is documented by the methane, alkalinity and dissolved sulfate distribution in pore fluids of the sediments from Site 684.

The section recovered contains portions of late Miocene, middle Pliocene, and late Quaternary records of the coastal upwelling regime with

alternating periods of hemipelagic and current-dominated deposition. It may contain some equatorial watermass signal. The sediments undergo early diagenesis affected by an influx of highly saline pore fluids, which promotes the widespread formation of dolomite and calcite.

SITE 685 (5070 m water depth)

A major tectonic boundary at the front of the Peruvian convergent margin abruptly juxtaposes the seaward end of the continental crust against the landward end of the accretionary complex. Sites 683 and 685 were placed on either side of this boundary to establish its nature and to date the beginning of accretion. From all indications, cores from Site 685 contain accreted sediment of late Miocene age, which is separated by a hiatus of 4.3 m.y. duration from overlying slope deposits of Pleistocene age.

The two main lithologies represented in the 468 m cored were divided into two lithostratigraphic units. Unit 1 (0 to 203.6 mbsf) consists of slope deposits. Within Unit 1, the interval from 0 to 80 mbsf is composed of diatomaceous mud with small oceanward-dipping normal faults, overlying a diatomaceous mud (80 to 200 mbsf) with variable bedding, folding, locally developed fissility, and a fabric that cuts the beds at high angles. Microfossil assemblages are of Pleistocene age, and most were transported from shallow-water environments on the shelf with lesser transport from upper and intermediate slope areas. The age range is well constrained and yields a surprisingly high rate of sedimentation, i.e., 100 m/m.y.

A hiatus with a minimum duration of 4.3 m.y. separates the lower Pleistocene Unit 1 from Unit 2 (203.6 to 468.6 mbsf) of early late Miocene age. The rocks are dominantly diatomaceous mudstones that are variably calcareous. In the upper part, relatively constant dips were observed, and the rocks showed a moderate to strong scaly fabric parallel to the bedding. Toward the bottom of the cored section the well-lithified parts are intensely fractured and show a strong scaly cleavage and a structure that can be related to compressional deformation. The apparent dips of bedding range from 45° to 60° , whereas those of the reflections in the seismic record are from 10° to 20° . Near the bottom of the hole are sedimentary breccias and sand. The breccia clasts have various ages from Eocene to late Miocene; some of the clasts show two generations of consolidation and erosion. The lower unit has the same characteristic transported fauna observed in the slope cover. Diatom assemblages show that the lithologic unit was deposited from 6.8 to 6.1 Ma. A minimum rate of sedimentation not corrected for tectonic thickening is about 250 m/m.y., but only about half of the thrust packet seen in the seismic record was penetrated.

Unusually steep gradients of chemical species dissolved in pore waters were characteristic of this site. The zone of sulfate reduction is very thin and thus methane generation begins at <11.6 mbsf. Methane gas hydrate was first recovered at 99 mbsf and was visually observed to about 165 mbsf. The depth of recovery is unusually shallow in this environment and may be linked with the early generation of the methane. Total-organic-carbon (TOC) contents are lower at this site than at the other sites drilled on Leg 112, perhaps because of dilution by rapid sedimentation. The maxima in alkalinity (156 mmol/L), phosphate (0.826 mmol/L), and ammonia (31.76 mmol/L) are the highest reported from deep ocean drilling. Despite the

extreme concentration gradients at this site, the amounts of diagenetic minerals (particularly carbonates and phosphates) that form per unit volume of sediment are small.

The stratigraphy and structure observed in cores from this site are consistent with the interpretations of the landward-dipping seismic reflections at the front of the Peru margin as an accreted complex. This confirmation from the cores is evidenced by the differing structural styles in sediment of the upper part of the slope cover and in sediment of the landward-dipping beds. The lower part of the slope cover appears to have been involved in tectonic deformation of the slope. The implied high rates of Miocene sedimentation in the accreted unit are consistent with deposition in a lower slope basin or the trench axis. Abundant microfossils transported downslope from the shelf are typical of lower slope basins and trench deposits. Therefore, all indications from the section drilled at Site 686 are consistent with the geophysical evidence for an accreted thrust packet. Its late Miocene age (6.1 to 6.8 Ma) indicates the time at which accretion began to prevail over other tectonic processes at the front of the margin.

SITE 686 (447 m water depth)

Site 686, at the southern end of the N-S transect along the Peru outer shelf, is located in the western Pisco Basin at a water depth of 446.8 m (Table 1; Figure 1). This site was selected to obtain a high-resolution record of upwelling and climatic history from Quaternary and possibly Neogene sediments, to calculate mass accumulation rates of biogenic constituents from an upwelling regime, and to document in detail early diagenetic reactions and products specific to the coastal upwelling environment.

Six lithostratigraphic units were defined, all of which are Pleistocene in age: Unit 1 (0 to 27.9 mbsf), Unit 2 (27.9 to 91.7 mbsf), Unit 3 (91.7 to 145.2 mbsf), Unit 4 (145.2 to 220.8 mbsf), Unit 5 (220.8 to 255.5 mbsf), and Unit 6 (255.5 to 303.0 mbsf). The sediments at Site 686 consist of diatomaceous mud in three major cyclic alternations, each cycle consisting of laminated (Units 1, 3, and 5) and bioturbated (Units 2, 4, and 6) intervals. Many bioturbated intervals contain silty, sandy, and shelly beds. The laminated intervals are more phosphoritic, containing layers of friable phosphate. Dolomites are common in all units except in Unit 1 between 0 and 16 mbsf, which consists of laminated diatomaceous mud with peloidal phosphorites. The major cyclic sequences in turn contain numerous smaller cyclic alternations between bioturbated and laminated diatomaceous muds. These cycles are best displayed in the physical index properties, i.e., water content, porosity and bulk density. It is obvious that this signal is due to textural changes. The cyclicity may record fluctuations in sea level and the concurrent changes in fine sand and silt influx. The laminated units probably represent periods of highstands of sea level and an expanded oxygen minimum zone. The smaller cycles appear similar in duration, amplitude, and chronostratigraphic position to Pleistocene oxygen isotope stages.

Diatoms could be grouped into floras indicative of strong-, intermediate-, and low-intensity coastal upwelling with oceanic character.

At least three prolonged phases of intense coastal upwelling appear coincident with Units 1, 2, and 3. Superimposed on these major and minor cycles is a clear trend of subsidence in the western Pisco Basin during the past 1.5 m.y. Benthic foraminiferal assemblages record four successively deeper habitats from a shelf edge (50-100 m) environment in early Pleistocene time to upper middle bathyal depths (500-1500 m) at the present time.

Diagenetic products are very common throughout the cores of Site 686. Single phosphate nodules are most abundant within the laminated units, but occur also as gravel layers within the bioturbated units. Lithified dolomite first appears at 18 mbsf.

Diagenetic reactions over the entire shelf and upper slope off Peru are influenced by the saline brine which extends throughout the subsurface over an enormous area. The diagenetic sequence of calcite formation followed by dolomitization, ubiquitous along the Peru margin, is recognized again at Site 686 and is reflected in maxima and minima of dissolved Ca^{2+} and Mg^{2+} profiles in interstitial waters. The subsurface brine, clearly seen in a chloride anomaly (132% of normal seawater), continually replenishes the interstitial water with Ca^{2+} and Mg^{2+} ions which are depleted by carbonate mineral formation. At Site 686 the brine contains large quantities of dissolved ammonia (>45 mmol/L) and phosphate (>0.08 mmol/L).

The sediments from Site 686 contain all components of a well-developed and variable coastal upwelling facies of Quaternary age. The sediment record is expanded in time, is continuous, and reveals low-temperature diagenetic reactions typical of organic-rich environments, particularly precipitation of dolomite and phosphate. These diagenetic reactions are strongly influenced by dissolved ion fluxes from a saline subsurface brine.

SITE 687 (306 m water depth)

Site 687 and the companion Site 686 (Table 1; Figure 1) bracket the critical range of water depth between 300 and 450 m near the lower boundary of the oxygen-minimum zone in the Peru coastal upwelling regime. These sites were selected to obtain a high-resolution record of upwelling and climatic history from Neogene and Quaternary sediments. The sediments at Site 687 consist of diatomaceous muds with large textural and compositional variations. These variations serve to subdivide the sediments into three lithostratigraphic units. Unit 1 ranges from 0 to 57.2 mbsf, Unit 2 from 57.2 to 102.5 mbsf, and Unit 3 from 102.5 to 205.7 mbsf. The boundary between Pliocene and Pleistocene sediments was established at 128 mbsf within Unit 3. The compositional variation in these units results from the occurrence of calcareous intervals and reflects different proportions of authigenic dolomite and calcite as well as biogenic (mainly foraminiferal and molluscan) calcium carbonate. The textural variation is due to sand and silt contents, which are higher at Site 687 than anywhere else along the paleoceanographic transect off Peru.

Benthic foraminifers support the water-depth changes inferred from the lithostratigraphy and in addition indicate low oxygen conditions for the deep habitats (300 m). The changes probably reflect eustatic sea-level

fluctuations during the Pliocene and early Pleistocene and basin subsidence during the middle and late Pleistocene.

In all sections, diatom floras were found to indicate different intensities of coastal upwelling and fertility, classified to represent (1) strong, (2) sporadic, (3) no upwelling but high productivity, and (4) normal continental-margin productivity. At least five prolonged phases of intense coastal upwelling and high productivity occur during shallow- and deep-water periods at Site 687.

Diagenetic products are very common throughout the cores of Site 687. Of these, friable phosphates occur only in the diatomaceous mud of Unit 1. Dense phosphate peloids are present throughout the lithostratigraphic units. Phosphate conglomerates are common at erosional contacts, and phosphate-cemented shells or bones were found in several cores. Authigenic calcite and dolomite are both abundant in the sediment as disseminated crystals in unlithified sands, silts, or muds, and as fully lithified nodules and beds.

Influence of a subsurface brine is clearly evident in a chloride anomaly equivalent to 140% of normal seawater salinity, as it was in the other shelf sites. Besides potentially supplying ethane, it continually replenishes Ca and Mg depleted by carbonate mineral formation.

The cores from Site 687 contain all components of a well-developed and variable shallow coastal upwelling facies of late Pliocene and Pleistocene age. The sediment record is condensed and reveals low-temperature diagenetic reactions typical of organic-rich environments, particularly of dolomitization. These diagenetic reactions are strongly influenced by the saline subsurface brine.

SITE 688 (3820 m water depth)

The three distinct sedimentary environments encountered in the 770 m penetrated at Site 688 record progressively deeper water sedimentation from early Eocene to Pleistocene time. The first lithostratigraphic unit (Unit 1; 0 to 338.5 mbsf) consists of bioturbated Pleistocene diatomaceous muds. Common terrigenous turbidites in the top 66 m indicate shelf-derived sediment input. An incipient fissility is developed in the Pleistocene section from 100 mbsf. Within the diatomaceous muds, benthic foraminiferal assemblages are representative of present water depths. Biostratigraphic data indicate sedimentation rates of around 300 m/m.y. for this part of the Pleistocene.

The second major sedimentary unit (Unit 2; 338.5 to 593.0 mbsf) comprises diatomaceous and diatom-bearing muds of early Miocene to Pliocene Pleistocene age. Fissility becomes better developed from 339 mbsf. A hiatus separating the Pleistocene and Pliocene is recorded between 341 and 350 mbsf in Hole 688A and between 350 and 356 mbsf in Hole 688E. Finely laminated sediment of alternating diatomite and mudstone with associated minor phosphorite is present in the upper Miocene and in the Miocene-Pliocene transition. These lithologies are similar to those of the contemporaneous sediments of the onshore Pisco Basin. Upper-mid bathyal benthic foraminiferal faunas indicate deposition of the Miocene-Pliocene

sequence in substantially shallower water (500 to 1500 m) than the present depths. Throughout the Miocene-Pliocene sequence, pervasive soft-sediment deformation is evident. Sedimentation rates for the Miocene-Pliocene section are approximately 23 m/m.y.

A marked lithological break to diatom-free calcareous sediment rich in terrigenous clastic detritus occurs at 593 mbsf between lithostratigraphic Units 2 and 3 (Unit 3; 621.5 to 769.5 mbsf; no recovery between 593 and 621.5 mbsf). This break coincides with a hiatus which spans the middle Eocene to the earliest Miocene, a period of approximately 21.5 m.y. The sediments recovered from 593 mbsf to 659 mbsf are predominantly greenish gray to dark greenish gray, poorly sorted quartzo-litho-feldspathic sandstones cemented by carbonate, which are interbedded with sandy siltstones and black mudstones. Benthic foraminiferal assemblages for this section indicate a middle and upper bathyal (150 to 500 m) range of water depths. The lower Eocene sequence from 678 to 769.5 mbsf includes abundant transported plant matter, coarse pebbly layers, and bioclastic material. Toward the base of this unit, calcareous mudstones and sandstones and silty, bioclastic limestones contain well-preserved molluscs, some of which are still articulated. They indicate little transport prior to deposition. Benthic foraminiferal and calcareous nannofossil assemblages indicate shelf depths for the deposition of this sequence. The oldest sediments recovered from 764 to 769.5 mbsf are of early Eocene age and comprise interbedded sandstones, siltstones, and mudstones with abundant plant material and foraminiferal assemblages indicating shelf depths. Sedimentation rates for the Eocene section are approximately 12 m/m.y. and are consistent with breaks between the pulses of sedimentation present.

Site 688 provided the most extreme geochemical gradients of Leg 112. Maximum values of alkalinity, ammonia, and phosphate exceeded previous records for DSDP or ODP sites. It was predicted that the methane generated in these sediments would be present in the gas hydrate phase, and Site 688 provided one of the best-documented occurrences of gas hydrates to date.

The hiatus at 350 mbsf marks the boundary between the signals from two very different bodies of interstitial water. Best seen in the chloride profile, a distinct freshening of the water is observed below this level. The freshening may indicate dilution by water originating at depth from dewatering of an accretionary complex or subducted sediments.

DRILLING SYNTHESIS

TECTONIC SUMMARY

NORTHERN CORRIDOR

Regional Setting. During ODP Leg 112, drilling was concentrated in two corridors previously surveyed with geophysical techniques and sampled by conventional means (Hussong et al., 1985). The northern corridor, near 9°S off central Peru, was cored at three ODP sites (684, 683, and 685; Figure 1) to constrain seismic interpretations. These sites are seaward of two industry drill holes (Delfin and Ballena) and landward of two DSDP sites (320 and 321) on the Nazca Plate. The morphology of the wide north-central continental shelf, and that of the slope, are typical of the Andean margin. This shelf is underlain by the coastal Salaverry and outer-shelf/upper-slope Trujillo basins (Thornburg, 1985). The upper continental slope is underlain by the Yaquina Basin. The upper-slope morphology ends at water depths between 3000 to 4000 m along a locally steepened scarp-like feature above the mid-slope terrace, a feature of broad regional extent (Prince et al., 1980; Bourgois et al., 1986). Below this terrace, the lower slope descends at a relatively constant dip to the flat floor of the Peru Trench. Seaward of the trench, the surveyed corridor includes an 850-m-high ridge subparallel to the trench axis, which is beginning to be subducted. Consequently the trench floor is locally constricted by this collision (Bourgois et al., 1986).

This morphology reflects a range of tectonic structure transitional between rapid deformation along the trench to more stability in the coastal area. The shelf is principally underlain by the coastal Salaverry Basin, a little faulted syncline. The adjacent Trujillo Basin, which straddles the shelf edge, is cut by many small faults of limited displacement (Thornburg, 1985). The landward flank and center of the basin were sampled from the Ballena and Delfin exploration drill holes (Figure 2) revealing an Eocene to upper Miocene continental-shelf sedimentary sequence above an erosional surface on Paleozoic metamorphic basement (Kulm et al; 1985; Schrader and Cruzado, pers. comm. 1986). A low basement ridge that crops out locally on the upper slope separates the Trujillo and Yaquina basins. The Yaquina Basin, with a depocenter in the middle of the upper slope, is cut by numerous normal faults on its landward flank (von Huene et al., 1985), which break the seafloor in a zone of anastomosing scarps observed in Seamarc II images (Hussong et al., 1985).

The mid-slope terrace is associated with a major tectonic boundary near the front of the Peruvian margin which juxtaposes continental crust against the accretionary complex. Although the structure of this boundary is poorly imaged in all mid-slope seismic reflection data (von Huene et al., 1985) it has tectonic significance because the disparate tectonic environments on either side indicate that a large segment of transitional crust is now missing (Figure 2). The accretionary origin of sediment at the front of the margin is evidenced by thrust packets adjacent to the trench floor and in the numerous landward-dipping reflections beneath the lower slope. The subduction zone is clearly marked in seismic records by thick stratiform sequences (Kulm et al; 1981; von Huene et al; 1985) that represent subducted trench sediment. The Peru Trench is filled with

turbidites about 1 km thick (Kulm et al., 1981; Bourgois et al., 1986) below which is a layer of hemipelagic and pelagic sediment above the igneous oceanic crust.

Prior to Leg 112, studies of the geophysical data and reports of industrial drill holes indicated that the same continental crust exposed along the coast, on offshore islands, dredged from outcrops, and drilled at the edge of the shelf could be geophysically extrapolated across the upper slope to the mid-slope terrace. This basement is unconformably overlain by sediment of Eocene and younger age deposited subsequent to a period of orogeny and uplift during the late Paleocene and Eocene, when vast areas of the Peruvian margin were subaerially exposed (summarized in Thornburg, 1985). Since the unconformity at the base of the Eocene was once subaerial, the crust has subsided. The objectives at Site 683 at the distal edge of the Yaquina Basin included verification that continental crust extends this far seaward and has subsided. This objective was coupled with those of a site across the tectonic boundary separating the two types of crust. The objectives at Site 685, just below the mid-slope terrace included verification of accretion and establishing the time when this process started. Thus the two types of crust could be compared. Site 684 at the edge of the shelf was drilled to obtain a Quaternary paleoceanographic history. This site reached middle Miocene sediment and thus provided a stratigraphic tie to the industry holes Delfin and Ballena in the Trujillo Basin (Figure 2).

Tectonic and Stratigraphic History. The time-stratigraphic history revealed by Leg 112 drilling along the northern corridor provides a tectonic framework for the north-central Peruvian margin since Eocene time. Eocene rocks were drilled at Site 683 and were recovered in clasts of a sedimentary breccia at Site 685. In seismic record CDP 2 the Eocene section can be followed from Site 683 landward across the upper slope to the basement ridge separating the Yaquina and Trujillo basins (Figure 2). The Eocene section is thick in the Delfin drill hole and is absent on the basement ridge penetrated by the Ballena hole; Eocene sediments do not extend shoreward beneath the Salaverry Basin. The distribution of the Eocene sediments was controlled by the subaerial basement topography with sediment transport from the east, trapping of the coarse fraction in the Trujillo Basin, and restricted outlet over a sill along the seaward basin flank. The muds which spilled over the sill were distributed uniformly over a gentle slope without much topography that forms the floor of Yaquina Basin. Following the Eocene these basins subsided, and by the end of middle Eocene time, Site 683 was probably on an upper slope. The long hiatus between Eocene and middle Miocene time extends across the Yaquina Basin and is a regional feature on land (Sanchez and Cruzado, pers. comm., 1986). After the hiatus, middle Miocene sedimentation resulted in another sequence of uniformly thick (>200 m) mudstones across the Yaquina Basin. A similar thickness was deposited in the Trujillo Basin. The Miocene benthic foraminifers at Site 683 indicate a depth in the lower bathyal zone, and those in sediments at Site 684 indicate a middle and upper bathyal zone. These relative depths and the uniform thickness of the middle Miocene sediments suggest a gentle slope between the sites.

At the front of the Peru margin the oldest accreted sediment was deposited during the late Miocene; the late Miocene is represented by a

break in sedimentation on the upper slope. Sedimentary breccias in the accreted sequence containing components of Eocene, early Miocene, and middle to late Miocene age show that a slope sequence of this age was exposed in late Miocene time. The sediment was accreted sometime during the 4.3-m.y. hiatus between its deposition and the accumulation of the discordantly overlying slope deposits.

The Pliocene and Quaternary sediments are thick in the Salaverry Basin, relatively thin in that part of the Trujillo Basin at the edge of the shelf, and thickest on the continental slope in the Yaquina Basin (Figure 2). Following sedimentation in the Miocene, sediment ponded in the coastal Salaverry Basin, but was eroded from the section of the Trujillo Basin at the edge of the shelf. Much of the sediment bypassing and eroded from the shelf edge was deposited in the Yaquina Basin on the upper slope. The observations from Leg 112 cores and the exhumed basement cropping out along the ridge between the Trujillo and Yaquina basins (Thornburg, 1985; Thornburg and Kulm, 1981) indicate uplift of the ridge into the zone affected by fluctuating high- and low-energy environments from variations in sea level.

Observations from drilling and geophysical surveys in the northern corridor indicate the following general tectonic history. In early Eocene time, the Peruvian landmass extended far seaward of the present coast, at least to the position of the present mid-slope area. During the middle Eocene the seaward part of the landmass became submerged, and sediment filled much of the Trujillo Basin, overtopped the silled margin, and spread into today's Yaquina Basin. An Oligocene hiatus on the margin, which is widespread throughout the Peruvian coastal area, corresponds with an eastward shift of the magmatic arc and volcanism to the Western Cordillera of the Andes. This must have been caused by a shift in the position or configuration of the subduction zone. Through continued subsidence the base of the upper slope was at lower bathyal water depths by middle Miocene time. Thus the seaward edge of the continent subsided at least 2 km during the early stages of the uplift of the Andes. This subsidence suggests a subduction zone dominated by tectonic erosion rather than accretion. Accretion began in late Miocene time, at the latitude of the northern corridor.

What then were the regional geologic and plate-tectonic conditions at the time (6 to 7 Ma) when the Andean margin changed from a non-accretionary to an accretionary margin? The Miocene was a time of increased sedimentation, as seen in the Leg 112 data. The rate of plate convergence was exceptionally rapid between 8 and 5 Ma (Cande, 1985). The Nazca Ridge was subducted at the latitude of the northern corridor (9°S) between 8.8 m.y. (Nur and Ben-Avraham, 1981) 7 m.y. (Cande, 1985). Thus we speculate that an increased quantity of sediment on the slope and in the trench axis, the increased rate of plate convergence, and the tectonic disruption caused by subduction of the Nazca Ridge may all have contributed to the change from a non-accretionary to an accretionary convergent margin.

SOUTHERN CORRIDOR

Regional Setting. During the Nazca Plate Project, an area at 11°S across the Lima Basin was studied extensively using multichannel seismics

(seismic line CDP-1; von Huene et al., 1985), single-channel seismics, and conventional sampling (Hussong and Wippermann, 1981; Kulm et al., 1981). This area was again studied to select drill sites for Leg 112 (Hussong et al., 1985). The geophysical survey that included Seamarc II and multichannel seismic techniques centered around multichannel seismic record CDP-1, and sampling included targets identified from Seamarc II images. Just prior to Leg 112, CDP-1 was reprocessed with stacking of twice the number of channels and migration (von Huene and Miller, unpubl. data). Although the sites selected for drilling are on three different seismic lines, they are projected into a generalized interpretation of CDP-1 that characterizes the area (Figure 3; Thornburg, 1985).

The morphology of the southern area differs from the northern in that it has a narrower shelf and three wide terraces on each of the upper, middle, and lower slopes (Figure 3). Beneath each terrace is a sediment-filled basin. Only the coastal Salaverry Basin is common to both the northern and southern corridors. The outer-shelf/upper-slope Trujillo Basin in the north is replaced by the upper- to middle-slope Lima Basin in the south. The division between upper and mid-slope is made at a low buried ridge (Figure 3). The lower-slope terrace is perched above a long lower slope that descends at a 12° dip to the trench axis. The Seamarc II image of the southern area shows ponded sediment on the terraces, outcrops of sedimentary strata, and normal faults on the ridges that separate them. On the lower slope, a series of regularly spaced linear ridges parallel the trench (Hussong et al., 1985). Morphology of the southern area is distinct from the northern area in two ways: (1) the greater depth of the Lima Basin, and (2) the adjoining middle slope ridge and terrace, which do not occur in the northern corridor.

The margin is constructed of normally faulted ridges that form barriers between basins (Thornburg, 1985). The lower slope is probably a zone of imbricate thrust faults spaced about 1 km apart (Hussong and Wippermann, 1981; Hussong et al., 1985). At its depocenter along the corridor, the Lima Basin contains about 1200 m of sediment of Miocene and younger age (Kulm et al., 1981). On the basis of benthic foraminiferal assemblages in dredged sediments, a subsidence rate between 275 m/m.y. and 500 m/m.y. was calculated for the Lima Basin (Kulm et al; 1981). Small normal faults are common on both the landward and the seaward flanks of the Lima Basin. Beneath the floor of the basin, seismic velocities are similar to those of continental crystalline basement onshore (Hussong and Wippermann, 1981).

The seismic reflection records made during the site survey (Hussong et al., 1985) reveal a profound unconformity beneath the Lima Basin. In reprocessed seismic records CDP-1 and Shell 1017 (von Huene and Miller, unpubl. data), the unconformity truncates steeply dipping beds, and reconstruction of the pre-unconformity structure indicates removal of possibly as much as 750 m of sediment. In CDP-1 this erosion is confined to a segment 60 km wide beneath the upper slope and terrace where the sediment fill of the Lima Basin is now thickest.

Tectonic and Stratigraphic History. The distribution of sites along the southern corridor provides stratigraphic control at both the seaward (Sites 682 and 688) and the landward (Site 679) ends. The litho- and biostratigraphy of the rocks drilled at the seaward end of the corridor

have many similarities to the onshore stratigraphy of the Peruvian coastal region. In particular, the Eocene recovered at Site 688 can be correlated with the Chira, Verdun, and Talara Formations onshore. The benthic foraminiferal assemblages, megafossils, and lithologies indicate proximity of high-energy environments and suggest a broad shelf and time transgression of the Eocene shoreline. The top of this Eocene section was also penetrated at Site 682, in the northern corridor, and similar Eocene rocks were dredged during the site surveys. The Eocene rocks recovered contain upper bathyal to shelf-dwelling benthic faunas. Above the Eocene is a major Oligocene hiatus that is as pronounced offshore as it is onshore. These stratigraphic similarities between the onshore and offshore areas are consistent with the seismic interpretations that continental crust extends almost to the front of the Peru margin. Prior to the Oligocene, the crust now at the front of the continental margin appears to have been part of the Peruvian shelf. The Eocene sequence at Site 688, which was then at shelf depths, is now 4.4 km deep. In seismic record CDP-1 the reflections from the continental-shelf sedimentary sequence penetrated at Site 688 extend to a point 15 km landward of the trench axis, where they are now about 6.2 km deep. Thus, at the front of the margin along the Lima Basin, subsidence of the continental crust has been the dominant factor of vertical tectonic movement during convergence and subduction of the Nazca Plate.

The landward stratigraphic control point, Site 679, provides a section that is readily correlated across the Lima Basin by seismic stratigraphy. Particularly significant is the hiatus at 245 mbsf between 7 and 11 Ma: when reflections from the hiatus are followed downslope, they become the profound angular unconformity that floors the Lima Basin. In CDP-1 the 60-km-wide angular part of the unconformity is buried under 1200 m of sediment deposited in a sequence of landward-migrating depocenters beneath the lower-slope terrace. The degree of angular discordance and the estimated 750 m of sediment eroded at the unconformity imply that the unconformity was subaerially exposed. The unconformity is 3.4 km deep at the present depocenter. Subsidence from a sea-level position at 6 Ma yields a rate of 490 m/m.y., a rate comparable to the 500 m/m.y. determined from benthic foraminiferal assemblages of sediment dredged from the seaward flank of the Lima Basin (Kulm et al; 1984). Thus the results from drilling on the landward flank of the Lima Basin corroborate those from dredging on the seaward flank. Consequently, the low buried ridge separating the upper and middle-slope terraces (Figure 3) formed an emergent barrier or insular platform composed of shelf sediment uplifted between middle and late Miocene time. Erosion of the insular platform supplied the abundant reworked and transported material in the middle and upper Miocene section recovered from Sites 682 and 688. Apparently, the Lima Basin area was uplifted during the late Miocene, eroded between 7 and 11 Ma, and subsided rapidly since about 5 Ma, when the sequence of Pliocene and Quaternary lens-shaped seismic packets accumulated in the landward-shifting sequence.

The upper Neogene plate-tectonic history indicates subduction of the Nazca Ridge in the area of the southern corridor between 7 Ma, when the southern flank of the ridge began to be subducted, and 2.5 Ma, when the trailing edge passed (Cande, 1985; Nur and Ben-Avraham, 1981). The period of accelerated plate convergence came between 8 and 5 Ma. Thus it seems that the subsidence of the Lima Basin occurred after accelerated

convergence and subduction of the Nazca Ridge. However, during the same period the Trujillo Basin appears to have been lifted, while the Salaverry Basin remained relatively stable with no more than 100 m of subsidence at the central position occupied by Site 680. The relation of plate-tectonic history to the history of vertical tectonism of these forearc basins is complex and must involve a variety of tectonic mechanisms.

PALEOENVIRONMENT OF SLOPE BASINS AND THE PERU COASTAL UPWELLING REGIME

The paleoenvironmental objectives of Leg 112 are intimately linked to the tectonic history of the continental margin, because the initiation of the eastern Pacific boundary current circulation and associated wind systems in the Miocene (a process which presumably established the coastal upwelling regime) coincided with a major tectonic phase triggered by the movement of the Nazca Plate underneath the South American craton. This event led to the development of the forearc basin system as it is arranged today. While the overall sedimentation history of the forearc basins reflects the vertical movements of the terrain that forms the foundation of the Andean margin, the sedimentary facies at the same time records the history of one of the best developed coastal upwelling regimes. As will be outlined below, the differential vertical motions of these basins through time, their position in different water masses along the steep margin, and the input of a biogenically dominated hemipelagic facies generate a wide range of chemical and sedimentological conditions for diagenesis. The expected normal extent of diagenesis in shelf basins of the Peru continental margin is surpassed by the effects from the incursion of a subsurface saline brine, which was discovered during drilling on Leg 112.

According to these different topics, the following summary of the results from Leg 112 that pertain to paleoenvironmental objectives is presented in three parts, entitled (1) Upwelling Oceanography, (2) Diagenesis, and (3) The Brine.

UPWELLING OCEANOGRAPHY

The paleoceanographic drill sites are located beneath the strongest wind-driven upwelling areas of the Peru Current regime. Today this region is situated along the upper continental slope at water depths between 150 and 500 m. The sites are arranged along a **north-south transect** (Sites 684, 679, 687, 686) and an **east-west transect** (Sites 681, 680, 679; Figure 1; Table 1). These sites straddle the critical depth range of the oxygen-minimum zone at the present sea level and at lower sea-level stands in the past (150 to 400 mbsl). Comparison of the sediment record along these transects provides criteria for a detailed identification of coastal upwelling signals needed for the reconstruction of water-column parameters (temperature, nutrients, oxygen), upwelling ecology (flora and fauna), and the interaction between shelf/slope morphology and currents of the Peru upwelling system (coastal current, poleward undercurrent). These studies will trace climatic and oceanographic forcing mechanisms through time and assess their effects on upwelling productivity.

The N-S transect. Four sites (684, 679, 687, 686), between 9° and 13°30'S at approximately 400 m of water depth (ranging from 306 to 450 m),

show that the Quaternary sediment record thickens enormously from 14 m in the north to >300 m in the south (Figure 4). This change is tectonically controlled. Sedimentation at the southernmost point (Site 686) reflects the subsidence of the western Pisco Basin, while the condensed record in the north implies vertical stability of a structural ridge at the outer shelf bounding the Trujillo Basin. Generally, the lower Quaternary sediments are usually more bioturbated, while the upper Quaternary sediments are laminated. The Pliocene/Pleistocene boundary at all sites coincides with the development of a shallow-water environment of outer-shelf character (50-150 m water depth). This is related to the onset of Pleistocene glaciation and sea-level lowerings. Such a coherent facies distribution over the length of the transect indicates that the sites, now located at the lower boundary of the oxygen-minimum zone at about 400 m water depth, must all have crossed this critical zone at least once. The observed variation in facies within these deposits must reflect that vertical transit.

Sites 679 and 687 show several alternations between bioturbated and laminated sequences; the section recovered at Site 686 contains at least 12 such alternations in the Quaternary. The latest Quaternary lithostratigraphic record is characterized by laminated diatomaceous muds at all sites, consistent with deposition of an upwelling facies at the present water depth. Studies concerned with latitudinal shifts of upwelling parameters, with location of the oxygen-minimum zone through time, and with accumulation estimates can rely on complete and representative sections along this N-S transect.

The Pliocene record recovered at the sites on the N-S transect shows the same latitudinal characteristics, except that this interval was not recovered at Site 686. As with the Quaternary, facies alternating between laminated and bioturbated diatomaceous muds indicate a long and continuous history of upwelling. An upper Miocene record was recovered only at Sites 684 and 679. The sparse diatom content at Site 679 indicates that during this time the site was located near the shore, probably at a water depth too shallow to preserve sedimentary signals of coastal upwelling. At Site 684 the Miocene section was deposited in slightly deeper water and thus contains better upwelling signals.

Each of the sedimentary records of upwelling in late Miocene, Pliocene, and Pleistocene-Holocene times along the upper Peru slope is probably of slightly different duration owing to local tectonics, but it is important to note that each such "upwelling time-slice" is bounded by bioturbated intervals attesting the integrity of the record. Within the reworked portions, though, the record becomes faint or is lost.

The detailed sedimentary records of upwelling obtained by drilling along the transects do not go back to the beginning of coastal upwelling along the Peru margin because of the subsidence and erosion of the middle Miocene upper slope. However, redeposited and transported sediments now preserved at the mid-slope area of the Lima Basin may contain a long-term record. Worth noting is the recovery of a slump block with upper Miocene laminated sediments at 400 mbsf at Site 688. Such a record contains a primary signal of upwelling comparable to the Quaternary record on the present upper slope, whereas the matrix contains the long-term history of upwelling.

E-W transect. Three sites were drilled at approximately 11°S representing a water-depth transect across the upper slope and outer shelf (Figures 5A&B; 679 = 450 m; 680 = 253 m; 681 = 151 m) of which Site 679 is the tie point with the N-S transect. The two shallower sites are located in the Salaverry Basin, while Site 679 is on the seaward flank of the structural ridge separating the Lima Basin from the Salaverry Basin. This structural ridge, which was subaerially exposed, confined the Salaverry depositional basin in the Miocene, where sediments were deposited in a restricted environment east of the ridge. Consequently, no Miocene upwelling record was ever present in the sediments deposited at these sites. The isolation of the Salaverry Basin continued throughout the Pliocene, and only since the beginning of the Quaternary period did strong coastal upwelling begin as a result of subsidence and rise in sea level. This record, however, is expanded, continuous, well-preserved and contains only minor amounts of terrigenous detritus. Thus it is an ideal record from which to reconstruct a high-resolution Quaternary upwelling history.

Shipboard investigations indicate that variations in the amount and type of organic matter, of the diatom flora, and of other indicators (see below) in these sediments seem to correlate with major glacial/interglacial cycles. The large amplitude of sea-level fluctuations during the Quaternary have not erased the upwelling record because tectonic subsidence during deposition maintained optimal water depth for its preservation. The record obtained at Site 686, at the southernmost end of the Lima Basin, is of the same quality and resolution as that at Sites 680 and 681, and the three sequences together will permit a most detailed study when improved chrono-, litho-, and biostratigraphic correlation has been established.

Cyclicity. Sediments laminated on a millimeter scale are present in the upper Quaternary sequences at Sites 680, 679, and 686. Shipboard studies on magnetic intensities, water content, wet-bulk density, porosity, and organic carbon revealed cyclic fluctuations of these properties over a scale of meters (Figure 6). Interbedding of laminated and bioturbated diatomaceous muds at even lower frequency (tens of meters) suggests alternations between a low-energy, low-oxygen depositional environment and high-energy environments with substantial terrestrial input and enhanced sediment reworking overlain by more oxygenated water. It appears that the apparent cyclicity in the upwelling facies off Peru is climatically forced. To recognize and evaluate high-resolution climatic signals were the most important objectives on which any of the anticipated studies of ancient coastal upwelling have to rely (Pisias et al., 1984; Imbrie et al., 1984; Martinson et al., in press). For this reason, we devoted some extra effort during shipboard work to delineate the frequencies of this cyclicity and to get a first impression of the causes and usefulness of these variations. Even though the ultimate evaluation must follow shore-based investigations, the results of the shipboard findings are of enough interest to be presented here.

At Site 680 the magnetic-intensity pattern of sediments shown in Figure 6 oscillates over the last 730 k.y. The implication is that alternations between input from terrigenous and "upwelling" sources control the abundance of magnetic carriers. A biogeochemical approach to the detection of cyclicity in the sedimentary record has been made on selected intervals from Site 680 in conjunction with magnetic and total-organic-matter

determinations. At present it is difficult to correlate all properties unambiguously, and it is evident that the cyclicity is not coherent in all properties studied at higher resolution. The same type of oscillations are shown in the physical index properties at Site 686. Again, these are thought to reflect the different lithologies dominated by either upwelling or terrigenous inputs. The consensus is that climatically controlled changes in the relative fluxes of major sediment components, i.e., organic matter and terrigenous detritus, are responsible for the observed alternations. At present, however, we cannot identify a uniform forcing mechanism, and it is not clear if and which parameters are leading and lagging in the cyclicity. Oxygen-isotope analysis on planktonic foraminifers from these intervals is planned to identify the primary climatic signal and then to relate the other cyclic variations to this reliable signal.

Upwelling signals. Diatom frustules and organic matter are by far the most abundant and pervasive biogenic components of the upwelling facies. Silicoflagellates, sponge spicules, and radiolarians were usually present, and calcareous nannoplankton was found occasionally. Planktonic and benthic foraminifers are concentrated in certain cores, where they may permit a detailed reconstruction of upwelling parameters, but usually calcareous faunal skeletons are rare.

The diatom record throughout the Quaternary indicates influence of warm- and cold-water masses at various times. In addition, the diatom assemblage commonly occurs in the form of monospecific assemblages indicative of blooms. Sites 686, 687, and 681, positioned underneath present-day upwelling plumes, contain the most detailed and best resolved diatom record. At these sites the floras indicate different intensities of coastal upwelling and associated nutrient availability. According to Schuette and Schrader (1979), these intensities can be classified as (1) strong upwelling, (2) intermittent upwelling, (3) no upwelling but high fertility, and (4) normal continental margin fertility. Various combinations and modifications of such qualitative upwelling character are manifest throughout the cores at these sites. The presently achieved resolution, however, is not sufficiently detailed to relate these phases to any of the observed cyclicities discussed above. At Site 684, the late Miocene upwelling environment is characterized by numerous blooms of diatoms and coccoliths intimately associated in laminations, the assemblages being indicative of high nutrient supply during brief and drastically alternating warm and cold phases. Perhaps the warm phases represent periods during which upwelling was seeded by equatorial waters, a phenomenon observed today only in abnormal oceanographic situations, such as El Nino conditions.

Of the planktonic foraminifers, five species indicating upwelling were identified, particularly in cores of the E-W transect. These are Globigerina bulloides, G. quinqueloba, Globigerinita glutinata, Neogloboquadrina dutertrei, and N. pachyderma. These same species were previously observed in plankton samples from surface waters of the Peru upwelling regime, where they display a distinct zonation around the centers of upwelling cells (Thiede, 1983). Their stable carbon- and oxygen-isotope composition should yield valuable information on water-column parameters. Also, as previously observed, certain genera develop abnormally small calcareous tests. While ecological reasons are at present unclear, a

connection to upwelling-water properties is suspected (Wefer et al., 1983).

Benthic foraminiferal assemblages, where present in sufficient numbers, record the successive habitats from outer-shelf to upper-bathyal depths during subsidence/eustatic sea-level fluctuations and, more importantly, may carry information on the bottom-water oxygen contents via their stable-isotope composition. With independent information from lithological data on sea-level fluctuations, these benthic assemblages should aid in differentiating tectonic from eustatic changes in water depths along the Peru upwelling regime.

Organic matter, measured in quantity and quality by pyrolysis and by various solvent extracts, seems the richest carrier of upwelling signals while being a most difficult one to unlock. Total-organic-carbon (TOC) contents vary widely between 12 wt% and 2 wt%. An indication of cyclicity in its burial was found at several sites as illustrated for Hole 680A in Figure 6. Dilution from terrigenous clastics and changing input from biological production combine to account for the observed changes. Detailed chronostratigraphy is needed to convert these data to accumulation rates which then should readily reflect absolute changes in primary production as a measure for upwelling variability. While the hydrogen and oxygen indices (HI and OI, respectively) derived from Rock-Eval pyrolysis indicate marine plankton as the overwhelming source of the sedimentary organic matter, these plankton also exhibit some interestingly high OI values. Interpreted conventionally, these might reflect past oxydative decomposition as they were preferentially found near unconformities. However, interpretation of this signature as an indication for terrigenous sources should be used with caution when applied to fresh organic matter rich in natural oxygenated organic compounds.

Attempts were made to recognize biomarkers derived from the major groups of primary producers contributing to the Peru coastal upwelling ecosystem in the sediment, as well as to establish the temperature regime under which the bulk of organic matter was synthesized, and the fate of labile compounds during diagenesis. Of particular interest is the preservation of organic pigments of the phaeophytin type, presumably derived from chlorophyll, and of the carotenoid type, which are both produced by phytoplankton. These pigments are present in Quaternary sediments at most of the sites. In a detailed downhole study made at Site 684, the pigment abundances vary with depth from Pleistocene to upper Miocene strata and correlate well with diatom and nannoplankton contents. On the same samples, lipid extracts were further assessed by gas chromatography in an attempt to document the distribution of long-chain alkenones, markers for algal input and algal growth in a certain temperature regime (Brassell et al., 1986). The most unexpected result is the observation that these organic molecules, which are believed to be synthesized exclusively by Chrysophyta (coccolithophorids), are abundant even in sediments devoid of nannoplankton skeletal remains. The inference is that either the nannoplankton record is grossly underrepresented off Peru owing to diagenetic dissolution or the alkenones have inputs other than from these algae. In any case, shore-based organic geochemistry on the molecular level may play a major role in the detailed characterization of the upwelling signatures encoded by the bulk organic matter, be they temperature specific or source specific.

DIAGENESIS

Decomposition of organic matter by anaerobic microbial remineralization (mainly by sulfate and carbonate reduction) is the dominant reaction mechanism observed in sediments at all sites during Leg 112. The sulfate-reduction zones extend downhole to various levels and are usually followed by zones of methanogenesis, except at sites where a brine replenishes the diminished interstitial sulfate reservoir from below. This exceptional phenomenon was observed at the shelf sites and will be discussed separately. The dominance of anaerobic sulfate- and carbonate-reduction reactions is due to the high amount of organic matter and the rapid rates of burial at all sites. The burial flux of organic matter is so large in comparison to the rate of decomposition that it represents an inexhaustible supply for microbial activity; hence these reactions are not substrate limited as is the case in other deep-sea sediments. Instead, the observed depth zonation of sulfate reduction and methanogenesis by microbial redox mechanisms are controlled by the type of organic matter, the bulk sedimentation rate, and the available electron acceptors. The reason for this situation is that the rate of consumption of interstitial sulfate by microbes is so rapid that diffusional supply of sulfate becomes the limiting factor. Early diagenesis along the Peru continental margin may therefore be considered a carbon-fueled and sedimentation-rate-controlled process.

Sulfate reduction and methanogenesis. Table 2 shows inferred bulk sedimentation rates from the interstitial-sulfate-reduction profiles of all sites compared to the rates estimated from biostratigraphy. There is a good agreement between these two methods of estimation, except that the rates based on sulfate reduction are larger by a factor of two. It is possible that the empirical relationship first established by Berner (1981) in nearshore environments and later expanded by Reimers and Suess (1983) to include hemipelagic deposition (Figure 7) is biased toward nearshore and shallow-water environments, or else that the sulfate-reduction rate is not a simple function of sedimentation rate. Another likely explanation for the discrepancy is that the rates based on biostratigraphy are inherently minimum rates, since they include, and in some cases amplify, small hiatuses.

The occurrence of methane at all sites drilled during Leg 112 is directly related to the disappearance of dissolved interstitial sulfate. It implies that the source of methane is microbial reduction of carbonate ions, an assumption which is in accord with the classic model by Claypool⁵ and Kaplan (1974). Methane is present in large amounts, on the order of 10^5 to 10^6 microliters of methane per liter of wet sediment, where sulfate ions are absent. These concentrations represent minima, because it is the upper limit of the amount of methane that can be retained by the sediment as it is brought on deck and decompresses to atmospheric pressure.

Just as the bulk sedimentation rate limits the diffusion of seawater sulfate into the sediment, so does the sedimentation rate limit the upward exchange of metabolites with the overlying seawater, causing excessive build-up of ammonia, phosphate, hydrogen sulfide, methane, and alkalinity within the pore water. This is responsible for the observed record concentrations of some metabolites, particularly at Sites 685 and 688. The

alkalinity, ammonia, and phosphate contents at these sites are the highest ever observed during DSDP and ODP drilling. Samples from this chemically extreme environment will allow the study a number of diagenetic processes in a detail not possible elsewhere. These studies include ion-exchange reactions involving ammonia, formation of sulfides, phosphates, carbonates, and gas hydrates.

Gas hydrates. Natural gas hydrates consist of a rigid framework (clathrate structure) of water molecules in which methane is trapped and effectively condensed. These solid substances form under specific pressure and temperature conditions that are encountered in hemipelagic sediments at depths of up to 1100 mbsf and in water depths greater than about 500 mbsf. The stability field depends on bottom-water temperatures, pressure, and methane concentration. Sediments at all four deep-water sites (Sites 682, 683, 685, and 688; Table 1) drilled during Leg 112 are within this stability field of gas hydrates. Solid pieces of gas hydrates were recovered (Figure 8) at two of the sites and are likely present at all four.

The properties of the observed gas hydrates analyzed on board indicate the predominance of methane over ethane in the hydrate structure. Based on the chloride and salinity values, a variable admixture of interstitial water or perhaps seawater from drilling that contaminates these samples was invariably detected.

During core recovery, gas hydrates dissociate into methane and water and are usually not recovered in solid form. As a result of dissociation, dilution of the interstitial chlorinities in relation to the amount of hydrate is observed and unambiguously signals the presence of gas hydrates in the subsurface. Such a dilution artifact was observed at all deep sites (682, 683, 685, and 688), with chloride values as low as 475 mmol/L (=88% of normal seawater chloride). The formation of gas hydrates is expected also to cause true chlorinity and salinity maxima owing to the exclusion of seawater ions from the clathrate structure. These maxima were indeed observed immediately above the zone of gas hydrate recovered at Sites 685 and 688 (100 and 140 mbsf, respectively), as well as at Sites 682 and 683, where hydrates were present but not recovered. Under conditions of lower sedimentation rates, the maxima are in communication with the sediment/water interface, so that diffusion tends to straighten out any gradients and thus prevent a build-up of dissolved ions above the concentration of normal seawater. Results from Leg 112 are the first to document such effects of salt exclusion during gas hydrate formation.

The actual distribution of gas hydrates within the sediment column is primarily controlled by the rate of methane production. Since production rates often decrease exponentially with depth, it came as no surprise that gas hydrates were found at relatively shallow depth, where methane had reached saturation concentrations. Below these levels gas hydrates became less abundant and eventually disappeared entirely before the base of the bottom-simulating reflector was reached. This might be part of the reason why the bottom-simulating reflector (BSR), usually assumed to be the transition from solid gas hydrates above to gaseous methane below, is discontinuous. The exact depth distribution of gas hydrates downhole was determined with the density, resistivity, and velocity logs at Site 685.

Calcite and dolomite. The intense sulfate reduction and methanogenesis encountered at all sites and the abundance of authigenic calcite and dolomite confirmed that the shallow and deep forearc basins along the Peru continental margin are excellent sites for examining the conditions that led to the formation of "organic" dolomites. "Organic" dolomites refers to the source of carbonate-ion formation via microbial or thermal degradation of sedimentary organic matter. Although it was not possible during shipboard work to obtain the stable-isotope composition and thereby identify the biogenic source of the carbonate ion, we obtained exciting interstitial-water data from closely spaced sampling to establish a reaction sequence for the complicated process of organic dolomite formation.

As sulfate reduction proceeds, the most important systematic downhole variations in dissolved calcium, magnesium, and alkalinity signal carbonate mineral reactions. In the first step, calcium profiles invariably show a distinct minimum, reflecting calcite precipitation. This causes the Mg/Ca ratio to increase and create a chemical environment highly favorable for dolomitization. At Sites 683 and 685 Mg/Ca ratios as high as 13 and 17 were measured; these are the most extreme values ever reported from non-evaporative environments. As a result of this increase in Mg/Ca ratio, dolomitization by calcite replacement reverses this trend until the Mg/Ca ratio drops below a value of 2 in the second step. Under these conditions calcite and dolomite continue to co-precipitate. Concurrent changes in alkalinity indicate whether direct stoichiometric precipitation occurs or whether replacement reactions dominate.

The distribution of both mineral phases observed in sequences of the shelf and deep-slope sites supports this reaction sequence. Both mineral phases begin to form within the sulfate-reduction zone, in some instances as shallow as 1 m below the seafloor (Site 687 at 0.7 mbsf, Site 681 at 4.2 mbsf); at the deep sites, carbonate precipitates only at comparatively great burial depths (Site 682 at 108 mbsf, Site 683 at 422 mbsf). Calcite generally precedes dolomite; disseminated rhombs in muds precede lithified beds or nodules. Both observations attest to the ongoing processes of carbonate mineral diagenesis.

The quantity of authigenic carbonates in the shelf sediments is higher than in slope sediments, however. The slower rates of sedimentation on the shelf may permit larger fluxes of dissolved calcium and magnesium to reach these layers at shallow subsurface depths, where carbonate mineral diagenesis takes place. The carbonate, calcium, and magnesium input may be enhanced by diffusion from the brine, which was discovered in the subsurface over the entire shelf area. Inversely, only small amounts of carbonate diagenesis account for the observed strong calcium and magnesium concentration gradients at the sites of high rates of sedimentation on the slope.

Baker and Kastner (1981) showed the necessity for sulfate depletion before dolomitization begins. Since 1981 it has become evident that dolomite formation in organic-rich sediments such as in the upwelling facies of the Peru margin is a diagenetic process (Baker and Burns, 1985; Suess et al., 1986) which inevitably follows sulfate reduction.

Phosphates. Authigenic phosphates occur in two forms: as friable lenses and laminae and as dense nodular gravel in hardgrounds. Both types are restricted to shelf and upper-slope sites. Friable phosphates occur mainly in laminated diatomaceous muds formed through regeneration of organically derived phosphorus. The nodular phosphates are complex entities formed through repeated cycles of burial, phosphatization, and exhumation. They are characteristic for condensed stratigraphic sections and commonly mark unconformable surfaces. The most favorable sites for phosphatization along the Peru margin are those shelf and slope regions which were, at least periodically, within the oxygen-minimum zone and which had low sedimentation rates. The deep sites, in contrast, lay below the oxygen-minimum zone and have enormously high sedimentation rates, and no phosphates were found. The low concentrations of interstitial dissolved phosphate at the shelf sites and the record high contents measured at the deep-slope sites support the observed distribution pattern of the solid phosphorite phases.

Iron and manganese. The carbon-fueled and sedimentation-rate-limited diagenetic process, as outlined above, has considerable implications for the metal content and distribution of the Peru margin sediments. Confining the metal-oxide reduction zone, another ubiquitous process in sedimentary decomposition of organic matter, usually referred to as sub-oxic diagenesis, chemically reduces most of the detrital metal oxides, which are dissolved and lost from the sediment before they are deeply buried. This process operates in the uppermost few centimeters of the sediment surface and affects manganese and iron in particular. The loss of magnetic signal from magnetite reduction in the uppermost sediments observed throughout Leg 112 is one consequence; another is the formation of metal sulfides and possibly of mixed carbonates. At Site 688 the magnetic signal reappeared at depth, perhaps owing to the formation of greigite and/or pyrrhotite. Metal carbonates of iron (siderite) and manganese (rhodochrosite) usually do not occur as pure phases and could not be found with shipboard techniques, but they form solid solutions with the carbonates of calcium and magnesium: i.e., calcite, dolomite, and ankerite.

Geomicrobiology. The major assumption on which is based the scheme of early diagenetic processes outlined above infers that anaerobic microbial activity is operating to a depth of at least 200 mbsf (Whelan et al., 1986). This view is not shared by all sediment microbiologists. During Leg 112 a major sampling effort was devoted to documenting microbial activity to depths much below the several meters usually accepted as the lower limit of the active biosphere. No abiological processes, such as redox reactions or dissociation, are known that could explain the observed interstitial-water profiles. Advective or diffusive transport, however, are mechanisms which affect subsurface fluids in marine sediments but are rarely encountered and would not explain the observed methane and sulfate distribution patterns. The discovery of a subsurface brine at the shelf/basin sites during Leg 112 must be considered a very fortunate circumstance. The same sites were extensively sampled for the geomicrobiology project, i.e., Holes 679C, 680C, and 681C along the E-W transect (Figure 5). Interstitial sulfate and methane differ considerably in depth profiles from one site to another. Hence microbial populations, while likely generally similar, might differ enough to yield convincing results on the deep microbial activity. Sulfate reducers should currently dominate all depth intervals at Sites 679

and 680 and the upper part of Site 681. Methanogens should dominate in the interval from 30 to 90 mbsf at Site 681. Below this interval, however, sulfate reducers might be active again owing to replenishment of sulfate from the subsurface brine. Even though the microbiology itself requires validation, the chemical evidence in itself is highly suggestive of extensive and persistent anaerobic microbial activity to considerable depths at the Peru margin sites and elsewhere.

THE BRINE

Strongly increasing salinity gradients in the pore fluids at all sites drilled on the shelf and upper slope off Peru indicated that a highly concentrated brine exists in depth not cored during Leg 112 (Figure 9). The maximum chloride content measured was 1043 mmol/L, which is equal to 188% of the value of normal seawater. The chloride gradients appear to be diffusion profiles between this highly concentrated solution and the less saline seawater. The depth of the strata containing the brine was not reached in any of the holes, although the steepness of the gradients indicates that at Site 684 we were closest to it. Chloride as a conservative tracer (because it does not participate in any reactions) can be used best to delineate the distribution of the brine over the Peru upper shelf and slope. The other dissolved constituents participate in various diagenetic reactions, and thus their distribution is primarily indicative of the origin and evolution of the brine during passage through the subsurface. The other major ions are calcium, magnesium, and sulfate, which participate in carbonate mineral diagenesis and sulfate-reduction processes, and phosphate and ammonia, which are accumulating in the brine as it passes through organic-rich sediments.

The dissolved sulfate and methane distributions at Site 681 demonstrate the importance which the brine exerts on early diagenesis (Figure 10). The high organic-carbon contents and the high rates of sedimentation at this site drive microbial sulfate reduction to completion at a depth of 27 mbsf, and a zone of methanogenesis develops below. At greater depth, however, beginning around 100 mbsf and within the zone of high salinity, sulfate is replenished from below, and methanogenesis again ceases. In that way three distinct zones of early diagenesis coexist, in each of which dolomitization and calcite formation are prevalent. It is expected that a distinct brine signature is present in the stable-isotope signature of these various authigenic carbonates.

A clear trend of decreasing sulfate and increasing ammonia and phosphate concentrations of the brine is seen at Sites 684, 686 and 687. Furthermore, the isohaline surfaces at neighboring Sites 686 and 687 follow time-stratigraphic horizons (Figure 5A). This is a peculiar phenomenon which needs closer examination. The ammonia and phosphate concentrations at these sites show a non-stoichiometric relationship to sulfate reduction and alkalinity, strongly suggesting preferred input of these metabolites. These observations may indicate subsurface flow of the brine below the depth intervals cored and diffusional transport above the lateral flow, as seems evident along the E-W transect.

At Site 679 the salinity distribution complicates the pattern of the subsurface distribution of the brine considerably. An initial small

chloride increase was observed at 30 to 50 mbsf, which then gives way to a chloride decrease below seawater chlorinities. At the bottom of Hole 679E only 62% of seawater chlorinity was measured, indicating that a body with freshwater influence exists at depth only 16 km west of the postulated brine. Figure 5B depicts the subsurface structure and the contouring of isohaline surfaces in this area. Our preliminary conclusion is that two contrasting hydrological regimes, separated by the outer-shelf structural ridge, may exist in the subsurface along the E-W transect.

As one possible scenario we envision that to the east of this structural barrier the upper Miocene sequence may be the source of the brine. To the west of the structural barrier a body of relatively fresh water exists in the same upper Miocene section. It is possible that the subaerial exposure of the outer-shelf ridge during late Miocene time caused a restricted basin to form landward, where the brine may have formed, and that this subaerial region was the recharge area for freshwater that penetrated into the seaward sequence of upper Miocene sediments to the west. Subsequent diffusion from the source depth of the brine in an unknown location to the east of Site 681 and probably from within the upper Miocene sequence established the presently observed salinity gradients. The subsurface structural ridge may at present act as a sill to the seaward propagation of the highly saline fluids, and only the uppermost, the least saline, portion may spill over seaward into the Lima Basin.

It is noteworthy that the isohaline surfaces are not confined to the stratigraphic horizons and cross-bedding surfaces. The obvious freshwater influence to the west obscures the exact path of the brine penetrating into the Lima Basin.

The areal extent of the subsurface brine discovered on the Peru shelf and upper slope is enormous. It stretches for more than 500 km over the area drilled during Leg 112. Its source remains speculative, but as a first hypothesis we may assume that it was formed in an evaporitic hydrological regime established during late Miocene time, when the outer-shelf structural ridges constricted open-ocean water circulation in the shelf basins. Other possibilities include incursions of saline fluids from one or several evaporitic basins on land, or dense brines forming in Holocene evaporitic systems on land and flowing oceanward in porous sedimentary zones. The brine's composition and its subsurface distribution exert a strong influence on early diagenetic processes along the margin and in particular drive the widespread formation of authigenic carbonates by stimulating sulfate reduction and providing calcium, magnesium, and carbonate in excess of normal fluxes; these factors also control phosphate diagenesis. The mode of transport of the brine through the subsurface may be by diffusion near its source and by flow at more distant locations. During transport the brine acquires high metabolite concentrations while passing through organic-rich sediments.

CONCLUSIONS

Drilling during Leg 112 verified that continental crust extends to within 15 km of the trench axis of the Peru-Chile Trench by recovering shallow-water shelf sediment of Eocene age at Sites 682, 683, and 688. These sites are located in water depths of 3790, 3070, and 3820 m, respectively. During convergence of the Nazca Plate and the continental plate of South America the continental plate subsided, indicating that erosion of the margin was the dominant tectonic mechanism in the period from Oligocene to late Miocene time (36 to 7 Ma). In the accretionary wedge the oldest accreted sediments recovered (Site 685) are upper Miocene diatomaceous mudstones, which were deposited in the period 6.8 to 6.1 Ma and accreted to the continent between 5 and 4 Ma. In the middle Miocene, oceanographic and morphological conditions led to the deposition of sediments produced in highly fertile upwelling waters over the entire margin segment studied. These sediments consist of diatomaceous muds and mudstones that accumulated rapidly (sedimentation rates > 100 m/m.y.) in 100 to 500 m water depth on the modern shelf and upper slope. Equivalent diatomaceous mudstones were found in upper Miocene sediments at Site 688, at a distance from shore of 150 km and at a modern water depth of 3820 m. We may assume that the upwelling cells migrated landward in response to subsidence of the margin. The sediment cover on the entire upper and middle slope consists of reworked sediments from the primary depositional centers on the shelf.

The tectonic structure at the scale of the seismic records indicated transmission of horizontal compression only to the midslope of the margin. Tectonic structure at the scale of the cores also records the extent of the dominantly horizontal compressional structure as confined to the accretionary complex, i.e., the lower slope. Landward of the transition to continental structure the dominant deformation is non-compressional. The extent of the stress field has interesting implications for the mechanisms of tectonic erosion which seems to have occurred without a high degree of horizontal compressional stress.

We documented that the change from the erosional tectonic process to accretion coincided with the subduction of the Nazca Ridge. A similar concordance in time was seen between the change from uplift to subsidence of the Lima Basin at the time the Nazca Ridge was subducted.

There was considerable physical evidence for the migration of fluids through the sediments of the margin. Abundant water escape structures, which coincided with fault zones, appear to be major conduits in mudstones. At Site 688, we found a strong chemical signal from fluids that possibly originate from the subducting sediment, that is seen in seismic records about 4 km beneath the site.

The primary sedimentary signal of coastal upwelling is best preserved in Quaternary sediment of today's shelf and upper-slope area. Transects (N-S transect in 400 m water depth: Sites 684, 679, 687, and 686; E-W transect across the margin in 150, 250, and 440 m water depth: Sites 681, 680, and 679) show that Pleistocene upwelling deposits are affected by relocation of oceanic currents and sea-level fluctuations. Laminated diatomaceous muds occur only in the oxygen-minimum zone between 100 and 400

mbsl. The relative position of a particular site in, above, and below this zone through time results in alternations of laminated and bioturbated facies units, as recognized at Sites 679, 686, and 687. The distribution of hiatuses within the Pleistocene sequence can be used to estimate the glacially induced changes in the position of the poleward-flowing undercurrent. Tracking the fluctuations of the oxygen-minimum zone and the re-positioning of the current system are two of several approaches that will be taken to analyze and recognize climatic forcing of sedimentation on the Peru Margin.

Sediments from beneath coastal upwelling centers on the entire margin are rich in organic matter (1 to 12%) and experience extensive early diagenesis as a result of microbial degradation of this organic substrate. Organic carbon is oxidized by sulfate reduction and methanogenesis in all sections drilled, and the chemical environment thus produced promotes formation of diagenetic minerals, i.e., calcite, dolomite, francolite, chert, and sulfides. This normal sequence of microbial activity and diagenetic mineral formation in hemipelagic sediments is strongly affected by a hypersaline brine at sites on the shelf (679, 680, 681, 684, 686, and 687). The brine, which originates from some unknown depth in the subsurface of the shelf, replenishes sulfate in the interstitial waters and thereby suppresses methanogenesis.

REFERENCES

- Baker, P. A., and Burns, S. J., 1985. Occurrence and formation of dolomite in organic-rich continental margin sediments. Amer. Assoc. Petrol. Geol. Bull., 69, 1917-1930.
- Baker, P. A., and Kastner, M., 1981. Constraints on the formation of sedimentary dolomites. Science, 213, 214-216.
- Berner, R. A., 1978. Sulfate reduction and the rate of deposition of marine sediments. Earth and Planet. Sci. Lett., 37, 492-498.
- _____, _____, 1981. A new geochemical classification of sedimentary environments. Journ. Sediment. Petrol., 51, 359-365.
- Bourgeois, J., Pautot, G., Bandy, W., Boinet, T., Chotin, P., Huchon, P., Lepinay, B., Monge, F., Monlau, J., Pelletier, B., Sosson, M., and von Huene, R., 1986. Tectonic regime of the Andean convergent margin off Peru (SEAPERC cruise of R/V Jean Charcot, July 1986). C. R. Acad. Sci. Paris.
- Brassell, S. C., Eglinton, G., Marlowe, I. T., Pflaumann, U., and Sarnthein, M., 1986. Molecular stratigraphy: a new tool for climatic assessment. Nature, 320, 129-133.
- Cande, S. C., 1985. Nazca-South American Plate interactions since 50 my b.P. to Present. In Hussong, D. M., Dang, S. P., Kulm, L. D., Couch, R. W., and Hilde, T. W. C. (Eds.), Atlas of the Ocean Margin Program, Peru Continental Margin, Region VI: Woods Hole (Marine Science International), 14.
- Claypool, G. E., and Kaplan, I. R., 1974. The origin and distribution of methane in marine sediments. In Kaplan, I. R. (Ed.), Natural Gases in Marine Sediments: New York (Plenum Press), 99-140.
- Hartmann, M., Mueller, P., Suess, E., and Van der Weijden, C. H., 1973. Oxidation of organic matter in recent marine sediments. "Meteor" Forschungsergebnisse, C12, 74-86.
- _____, _____, 1976. Chemistry of late Quaternary sediments and their interstitial waters from the NW African continental margin. "Meteor" Forschungsergebnisse, 24, 1-67.
- Hartmann, M., and Nielsen, H., 1969. Delta ^{34}S -Werte in rezenten Meeressedimenten und ihre Deutung am Beispiel einiger Sedimentprofile aus der westlichen Ostsee. Geol. Rundschau, 58, 621-655.
- Hussong, D. M., Edwards, P. B., Johnson, S. H., Campbell, J. F., and Sutton, G. H., 1976. Crustal structure of the Peru-Chile Trench: 8°S to 12°S latitude. Amer. Geophys. Union Monogr., 19, 71-86.
- Hussong, D. M., and Wippermann, C. K., 1981. Vertical movement and tectonic erosion of the continental wall of the Peru-Chile Trench near $11^{\circ}30'\text{S}$ latitude. In Kulm, L. D., Dymond, J., Dasch, E. J., and Hussong, D. M. (Eds.), Nazca Plate: Crustal Formation and Andean Convergence. Geol. Soc. Am. Mem., 154, 504-524.
- Hussong, D. M., et al., 1985a. Atlas of the Ocean Margin Program, Peru Continental Margin, Region VI: Woods Hole (Marine Science Intl.), 19 pp.
- Hussong, D. M., et al., 1985b. Peru Margin Drilling Proposal. Unpublished Report, JOIDES/ODP Site Survey Data Bank, 44 pp.
- Imbrie, J., Hays, J. D., Martinson, D. G., McIntyre, A., Mix, A. C., Morley, J. J., Pisias, N. G., Prell, W. L., and Shackleton, N. J., 1984. The orbital theory of Pleistocene climate: support from a revised chronology of the marine delta ^{18}O record. In Berger, A., Imbrie, J., Hays, J., Kukla, G., and Salzman, B. (Eds.), Milankovitch and Climate, Part 1: Dordrecht (Reidel), 269-305.

- Kulm, L. D., Dymond, J., Dasch, E. J., and Hussong, D. M. (Eds.), 1981. Nazca Plate: Crustal Formation and Andean Convergence. Geol. Soc. Am. Mem., 154: 824 pp.
- Kulm, L. D., Suess, E., and Thornburg, T. M., 1984. Dolomites in the organic-rich muds of the Peru fore-arc basins: Analogue to the Monterey Formation. In Garrison, R. E., Kastner, M., and Zenger, D. (Eds.), Dolomites in the Monterey Formation and other Organic-rich Units. Soc. Econ. Paleont. Mineral. Spec. Publ., 41, 29-48.
- Kulm, L. D., Thornburg, T. M., and Dang, S., 1985. Drill hole stratigraphy dredge lithologies, and sample locations. In Hussong, D. M., Dang, S. P., Kulm, L. D., Couch, R. W., and Hilde, T. W. C. (Eds.), Atlas of the Ocean Margin Program, Peru Continental Margin, Region VI. Woods Hole (Marine Science International), 18.
- Kulm, L. D., Miller, J., and von Huene, R., in press. The Peru Continental Margin Record Section 2. In von Huene, R. (Ed.), Seismic Images of Modern Convergent Margins.
- Kvenvolden, K. A., and McMenavia, M. A., 1980. Hydrates of natural gas: a review of their geologic occurrence. U.S. Geol. Surv. Circ. 825, Arrington, 11 pp.
- Martinson, G. G., Pisias, N. G., Hays, J. D., Imbrie, J., Moore, T. C., and Shackleton, N. J., in press. Age dating and the orbital theory of the ice ages: Development of a high-resolution to 300,000-year chronostratigraphy. Quaternary Research.
- Nur, A., and Ben-Avraham, Z., 1981. Volcanic gaps and the consumption of aseismic ridges in South America. In Kulm, L. D., Dymond, J., Dasch, E. J., and Hussong, D. M. (Eds.), 1981. Nazca Plate: Crustal Formation and Andean Convergence. Geol. Soc. Am. Mem., 154, 729-740.
- Pisias, N. G., Martinson, D. G., Moore, T. C., Shackleton, N. J., Prell, W., Hays, J., and Boden, G., 1984. High resolution stratigraphic correlation of benthic oxygen isotopic records spanning the last 300,000 years. Marine Geology, 56, 119-136.
- Prince, R. A., Schweller, W. J., Coulbourn, W. T., Shepherd, G. L., Ness, G. E., and Masias, A., 1980. Bathymetry of the Peru-Chile continental margin and trench. Geol. Soc. Am. Map Chart Ser., MC-34.
- Reimers, C. E., and Suess, E., 1983. Spatial and temporal patterns of organic matter accumulation on the Peru continental margin. In Suess, E., and Thiede, J. (Eds.), Coastal Upwelling, Part B: Sedimentary Records of Ancient Coastal Upwelling: New York (Plenum Press), 311-345.
- Schuetter, G., and Schrader, H., 1979. Diatom taphocoenoses in the coastal upwelling area off western South America. Nova Hedwigia, 64, 359-378.
- Suess, E., 1976. Nutrients near the depositional interface. In McCave, I. N. (Ed.), The Benthic Boundary Layer: New York (Plenum Press), 57-80.
- Suess, E., Kulm, L. D., and Killingley, J. S., 1986. Coastal upwelling and a history of organic-rich mudstone deposition off Peru. In Brooks, J., and Fleet, A. J. (Eds.), Marine Petroleum Source Rocks: Geol. Soc. Spec. Publ., 24, 181-197.
- Thiede, J., 1983. Skeletal plankton and nekton in upwelling water masses off northwestern South America and Northwest Africa. In Suess, E., and Thiede, J. (Eds.), Coastal Upwelling: Its Sediment Record, Part A: New York (Plenum Press), 183-207.
- Thornburg, T. M., 1985. Seismic stratigraphy of Peru forearc basins. In Hussong, D. M., Dang, S. P., Kulm, L. D., Couch, R. W., and Hilde, T. W. C. (Eds.), Atlas of the Ocean Margin Program, Peru Continental Margin, Region VI. Woods Hole (Marine Science International), 16.

- Thornburg, T. M. and Kulm, L. D., 1981. Sedimentary basins of the Peru continental margin: structure, stratigraphy, and Cenozoic tectonics from 6°S to 16°S latitude. In Kulm, L. D., Dymond, J., Dasch, E. J., and Hussong, D. M. (Eds.), Nazca Plate: Crustal Formation and Andean Convergence. Geol. Soc. Am. Mem., 154, 469-508.
- von Huene, R., Kulm, L. D., and Miller, J., 1985. Structure of the frontal part of the Andean convergent margin. J. Geophys. Res., 90, 5429-5442.
- Wefer, G., Dunbar, P. B., and Suess, E., 1983. Stable isotopes of foraminifers off Peru recording high fertility and changes in upwelling history. In Thiede, J., and Suess, E. (Eds.), Coastal Upwelling: Its Sediment Record, Part B: New York (Plenum Press), 295-308.
- Whelan, J. K., Oremland, R. E., Tarafa, M., Smith, R., Howarth, R., and Lee, C., in press. Evidence for sulfate-reducing and methane-producing microorganisms in sediments from Sites 618, 619, and 622. In Bouma A.H., Coleman, J.M., Meyer, A.W., et al., Init. Repts. DSDP, 96: Washington (Govt. Printing Office), 767-775.

TABLE 1: Sites drilled during Leg 112

Site	Position (Latitude, Longitude)	Water depth (mbsl)	Drilled (mbsf)	Recovery (%)	Age of oldest sediment
679					
A	11°03.52'S 78°15.92'W	439.5	7.0	100.0	Holocene
B	11°03.80'S 78°16.34'W	450.5	107.2	96.1	Pliocene
C	11°03.81'S 78°16.33'W	450.5	75.5	92.4	Pliocene
D	11°03.83'S 78°16.33'W	439.5	245.4	47.1	late Miocene
E	11°03.78'S 78°16.34'W	462.0	359.3*	31.8	middle Miocene
680					
A	11°03.90'S 78°04.67'W	252.5	93.8	87.0	Pleistocene
B	11°03.90'S 78°04.67'W	252.5	195.5	50.4	early Pliocene
C	11°03.90'S 78°04.67'W	252.5	34.3	102.0	Pleistocene
681					
A	10°58.60'S 77°57.46'W	150.5	187.0	60.0	Pleistocene
B	10°58.60'S 77°57.46'W	150.5	143.5	67.8	Miocene(?)
C	10°58.60'S 77°57.46'W	150.5	91.4	98.7	Pleistocene
682					
A	11°15.99'S 79°03.73'W	3788.5	436.7	29.1	Eocene
683					
A	09°01.69'S 80°24.40'W	3071.8	419.2	52.2	middle Miocene
B	09°01.59'S 80°24.26'W	3071.5	488.0*	35.7	middle Eocene
684					
A	08°59.59'S 79°54.35'W	426.0	136.1	53.2	middle Miocene
B	08°59.59'S 79°54.35'W	426.5	55.0	67.6	Pliocene
C	08°59.59'S 79°54.35'W	426.5	115.0	48.8	middle Miocene
685					
A	09°06.78'S 80°35.01'W	5070.8	468.6	59.4	late Miocene
686					
A	13°28.81'S 76°53.49'W	446.8	205.7	88.3	Pleistocene
B	13°28.81'S 76°53.49'W	446.8	303.0	74.4	Pleistocene
687					
A	12°51.78'S 76°59.43'W	306.8	207.0	52.3	Pliocene
B	12°51.78'S 76°59.43'W	306.8	195.3	44.7	Pliocene
688					
A	11°32.26'S 78°56.57'W	3819.8	350.3	70.0	Pliocene(?)
B	11°32.26'S 78°56.57'W	3819.8	360.0*	0.0	
C	11°32.26'S 78°56.57'W	3819.8	359.8*	12.0	Pleistocene
D	11°32.26'S 78°56.57'W	3819.8	345.0*	0.0	
E	11°32.28'S 78°56.65'W	3825.8	769.5*	35.4	Eocene

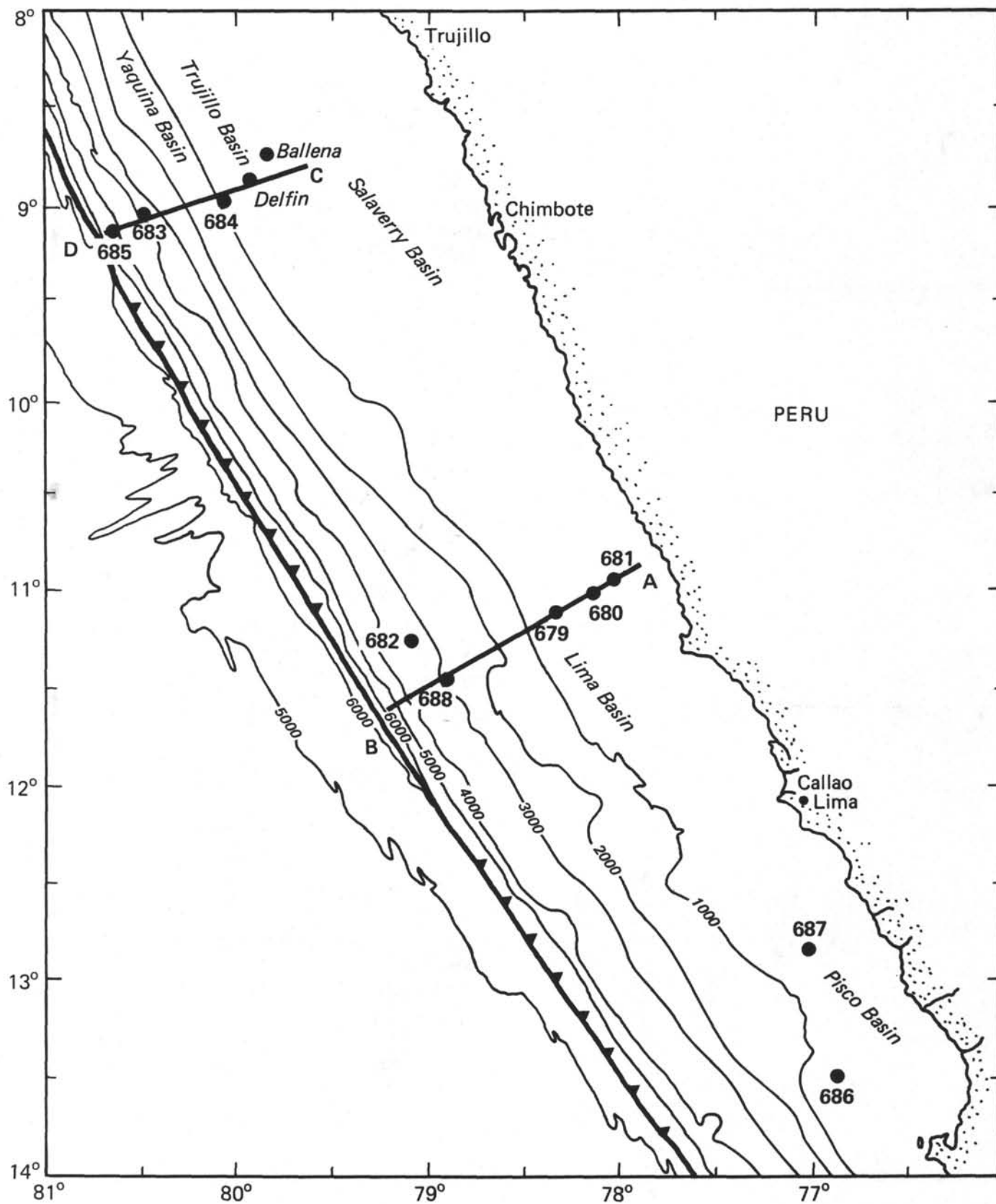
* Indicates that part of the hole was washed. The washed intervals were: Hole 679E, 0-245 mbsf; Hole 683B, 0-402.5 mbsf; Hole 688B, 0-360 mbsf; Hole 688C, 0-350.3 mbsf; Hole 688D, 0-345 mbsf; Hole 688E, 0-350 mbsf.

TABLE 2: Rate of sedimentation estimated from sulfate reduction as compared to biostratigraphically derived sedimentation rates

Site	Sulfate reduction (mmol/m)	Rate of sedimentation	
		Sulfate reduction (m/m.y.)	Biostratigraphy (m/m.y.)
679	0.15	20	12
680	0.90	100	55
681	0.93	140	80
682	0.40	40	26
683	1.76	180	110
684	1.47	150	35 (?)
685	2.23	250	130
686	2.26	255	160
687	1.07	105	65
688	4.12	300	150 - 350

FIGURE CAPTIONS

- Figure 1: Location of sites drilled during Leg 112 off Peru.
- Figure 2: Simplified structural transect based on seismic survey and results of Leg 112 across the Peruvian margin at 9°S. Included are results from industry holes Ballena and Delfin.
- Figure 3: Simplified structural transect based on seismic survey (Thornburg, 1985) and results of Leg 112 across the Peruvian margin at 11°30'S.
- Figure 4: Profiles of sedimentary sections recovered at Sites 684, 679, 687, and 686 on the shelf, which form a latitudinal transect. For locations see Figure 1. Individual sections are positioned according to water depth, and the lower boundary of the oxygen-minimum zone (400 mbsl) is indicated. Chloride concentrations are given for Sites 686 and 687 to outline the extent of the subsurface brine.
- Figure 5A: Generalized stratigraphic relationship of sediments recovered at Sites 679 (450 m water depth), 680 (252 m water depth), and 681 (150 m water depth), which form a transect across the shelf and upper slope off Peru. Isoclines of chloride concentration (in mmol/L) in interstitial waters outline the influence of the subsurface brine encountered in all sites drilled on the shelf. Note the freshening of interstitial waters observed in the lower section at Site 679.
- Figure 5B: Location of Sites 679, 680, and 681 on a structural profile of the shelf and upper slope (Thornburg and Kulm, 1981).
- Figure 6: Examples of cyclicity observed in sediments of Hole 680A, 680B, 686A and 686B. Physical properties, organic-carbon content, and magnetic intensity fluctuate in cyclic patterns that correlate with global climatic and sea-level cycles. The section is of Pleistocene age.
- Figure 7: Relationship of dissolved interstitial sulfate concentrations and sedimentation rates from Holocene marine environments (Reimers and Suess, 1983). The plot shows dissolved interstitial sulfate gradients and the bulk sedimentation rates of several marine sediments including three Peru margin piston cores (7706-39, -04, -36). Bar lengths represent uncertainties in the sedimentation rates. Data points labelled 10, 92, 47, and 79 are for sediments from northwest Africa (Hartmann et al., 1973, 1976). Two bars for one core represent Holocene and Pleistocene sections, respectively. The other data are for sediments from the Kieler Bucht (KB, Hartmann and Nielsen, 1969); Danziger Bucht (DB) and Bornholm Basin (BB) (Suess, 1976); Long Island Sound (FOAM), Saanich Inlet (SI), Chesapeake Bay (ChB), Somo Sound (SS), Santa Barbara Basin (SB), Pescadero Basin (PB), and San Pedro Basin (SPD) (Berner, 1978).
- Figure 8: Photograph of solid gas hydrate recovered in Section 112-688A-15X-7 at 141 mbsf.
- Figure 9: Gradients of chloride in interstitial waters of paleoenvironmental sites drilled on the shelf along the Peruvian margin.
- Figure 10: Sulfate and methane abundances in interstitial waters at Site 681.



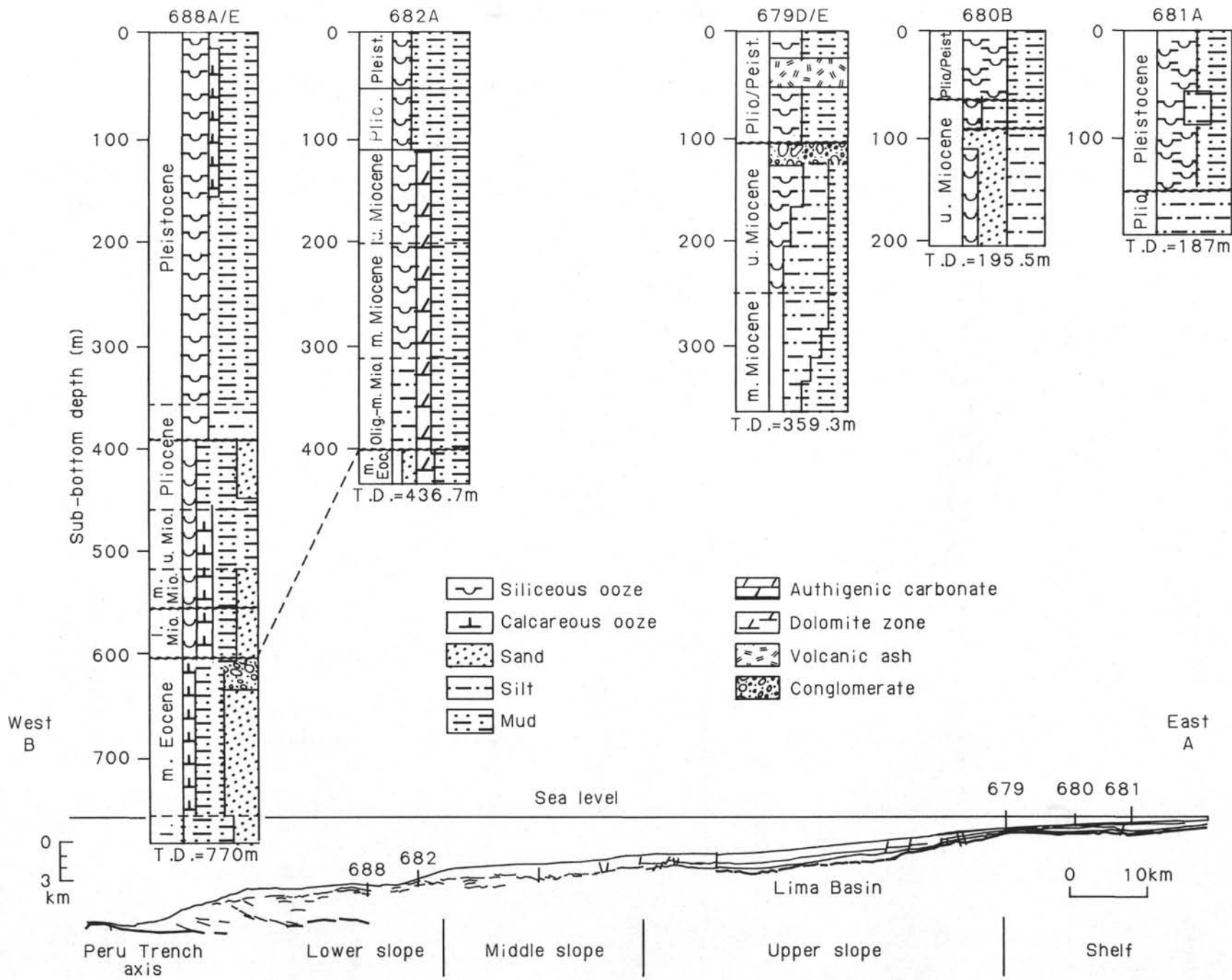
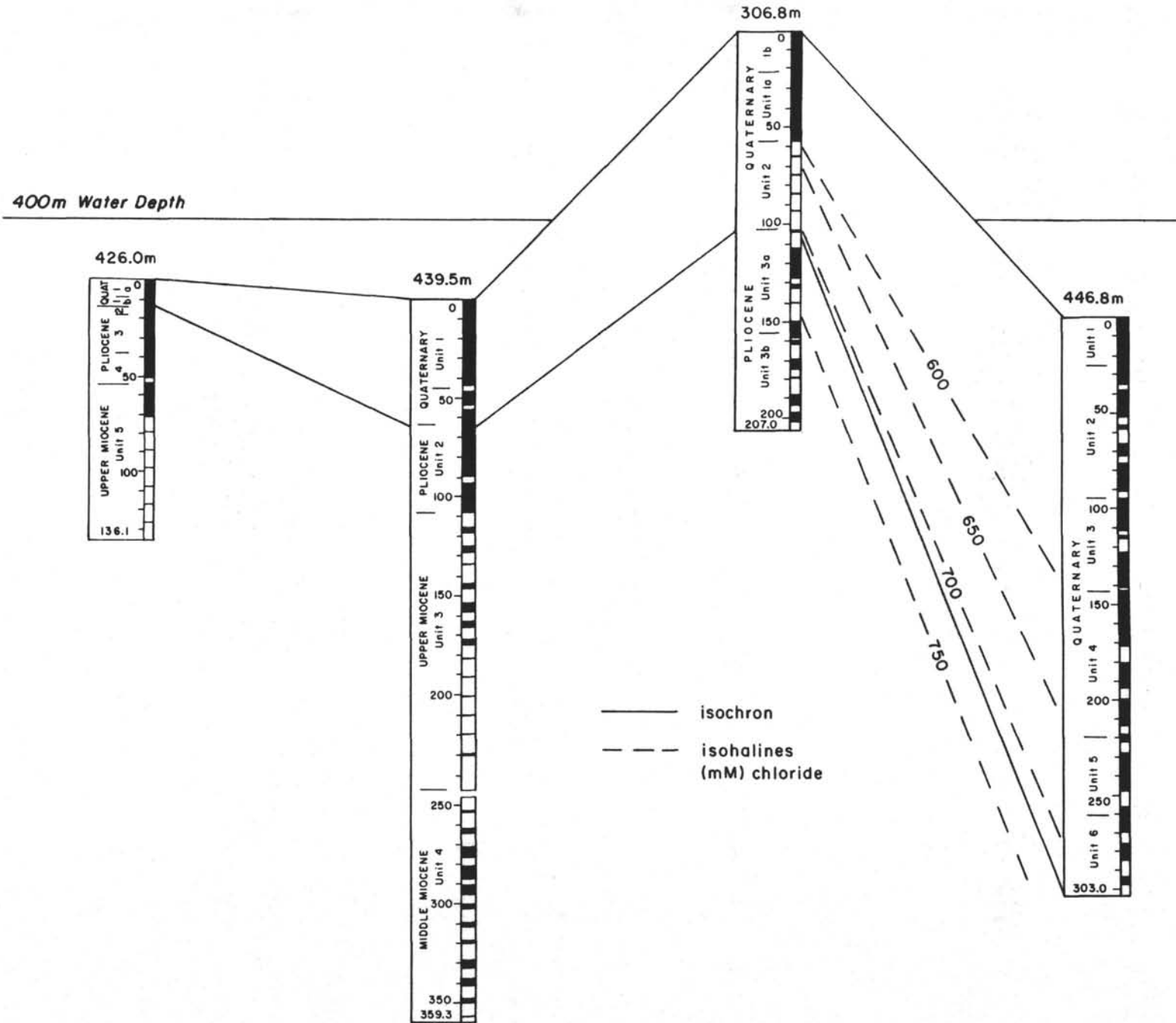


Figure 3.



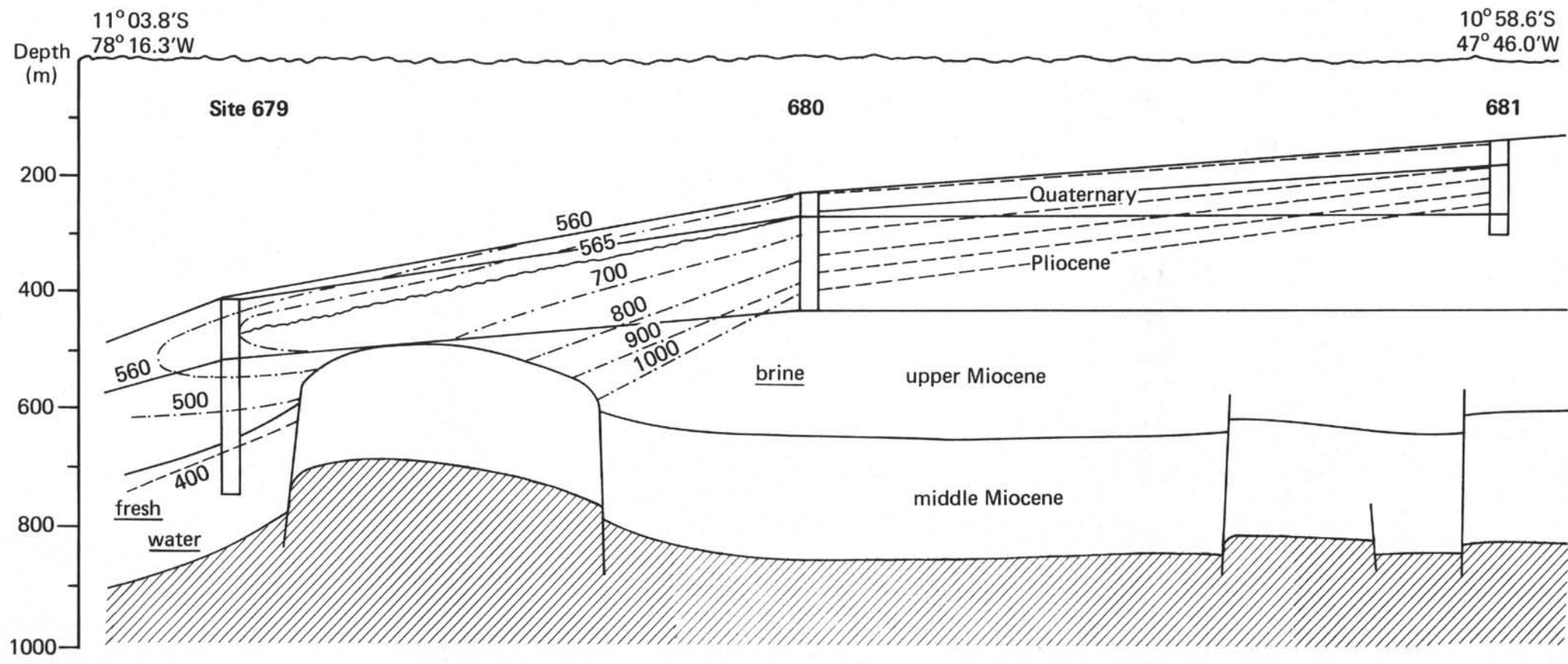


Figure 5A.

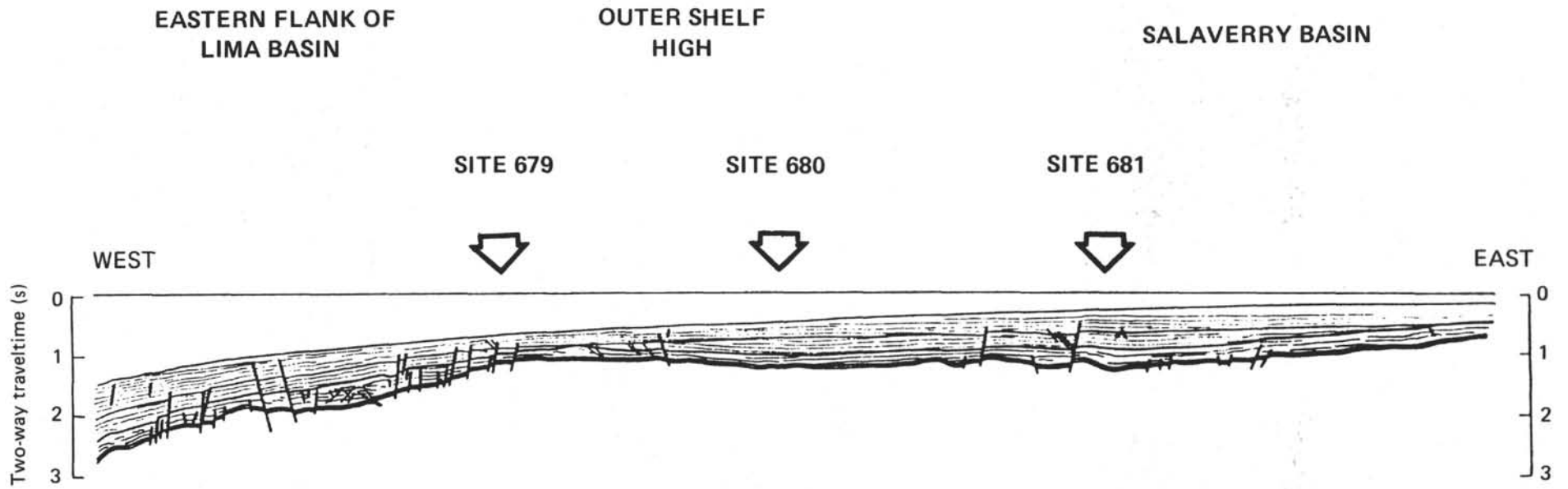
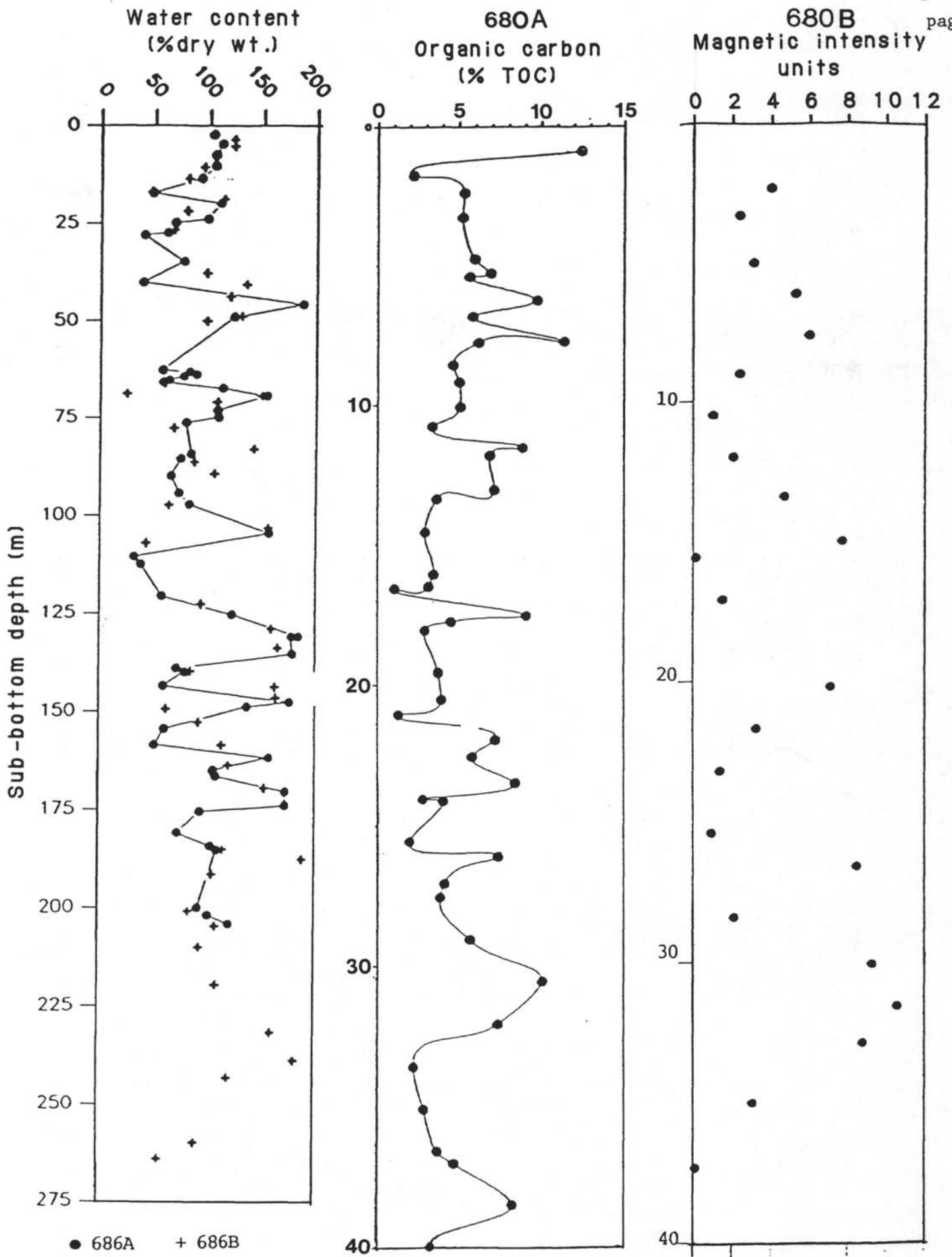
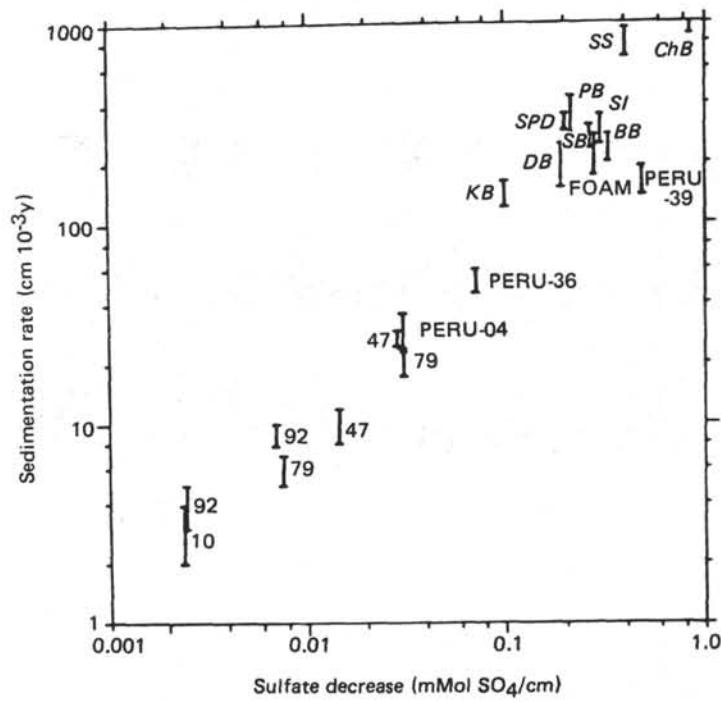


Figure 5B.

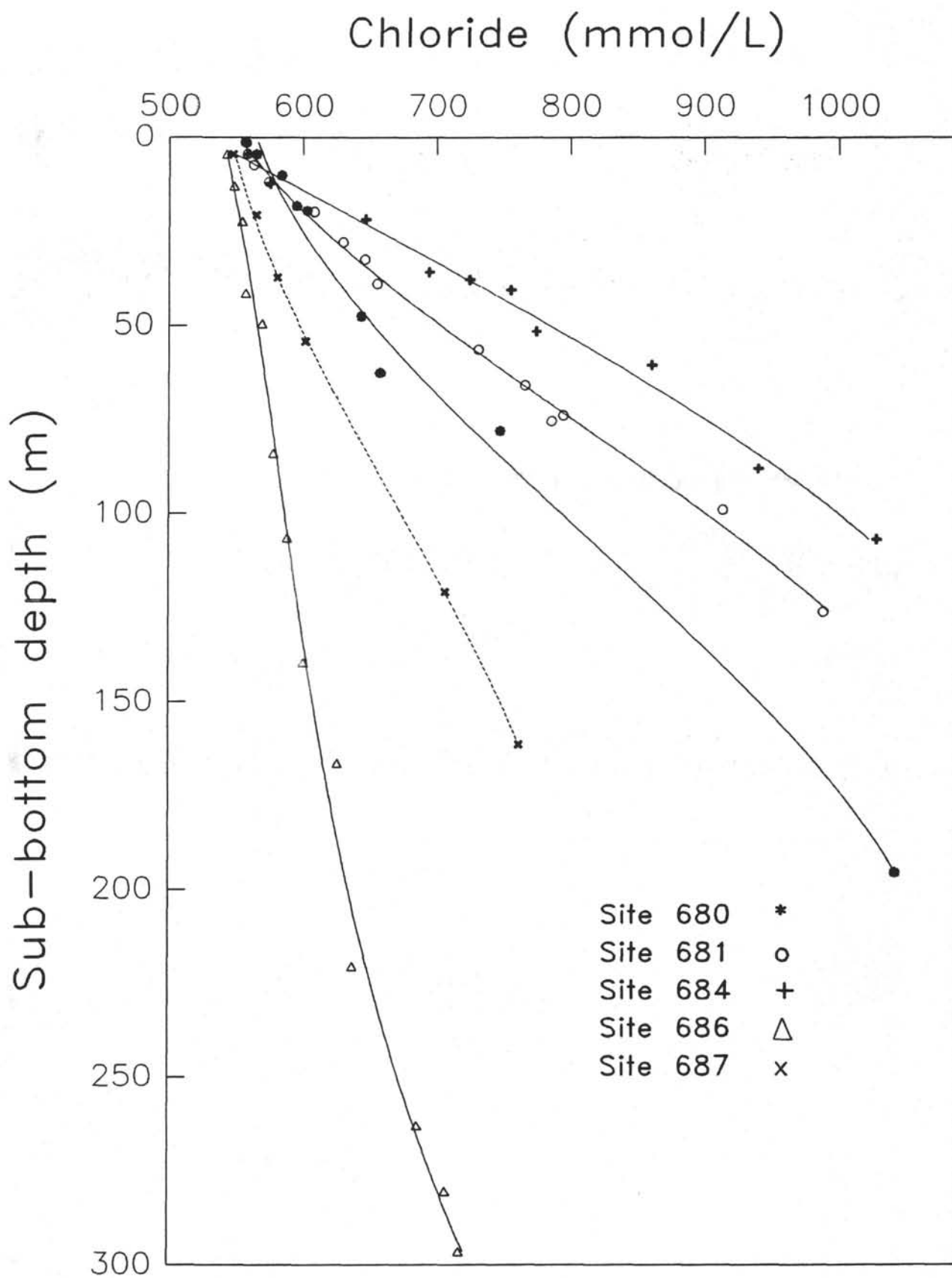




page 47

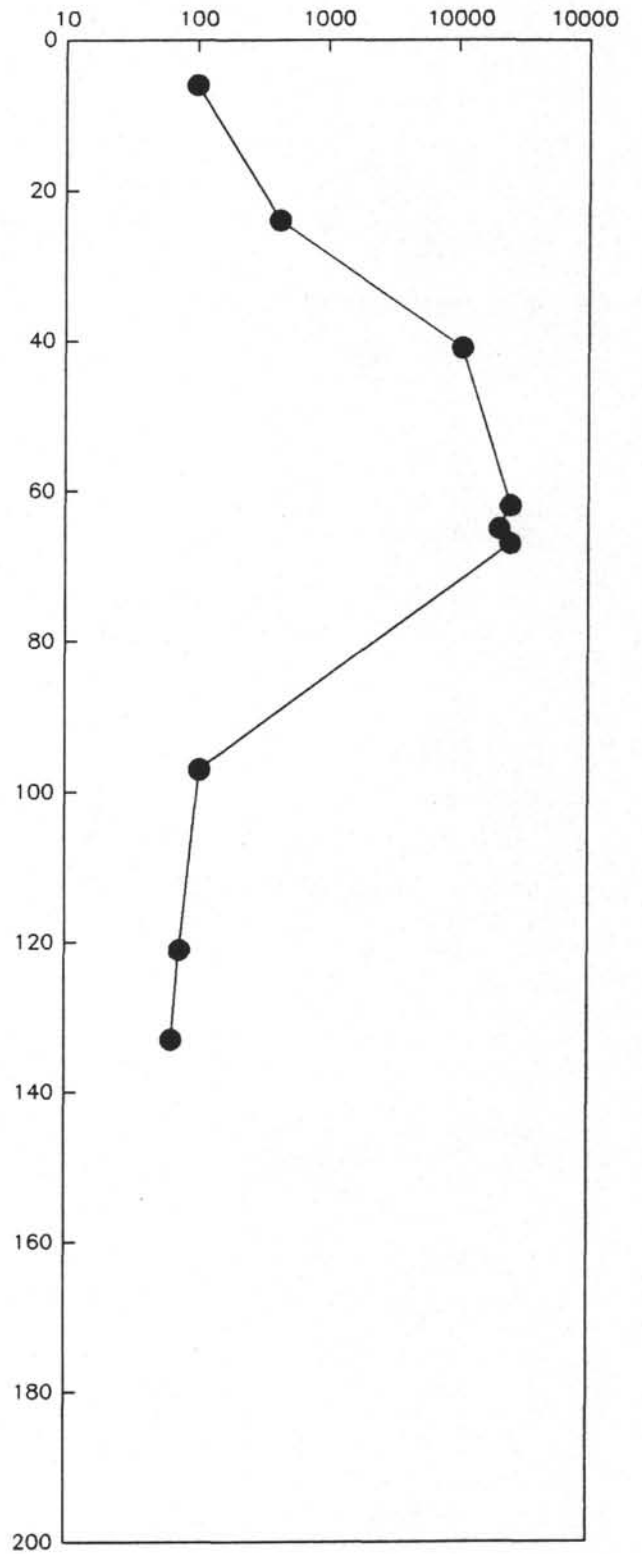
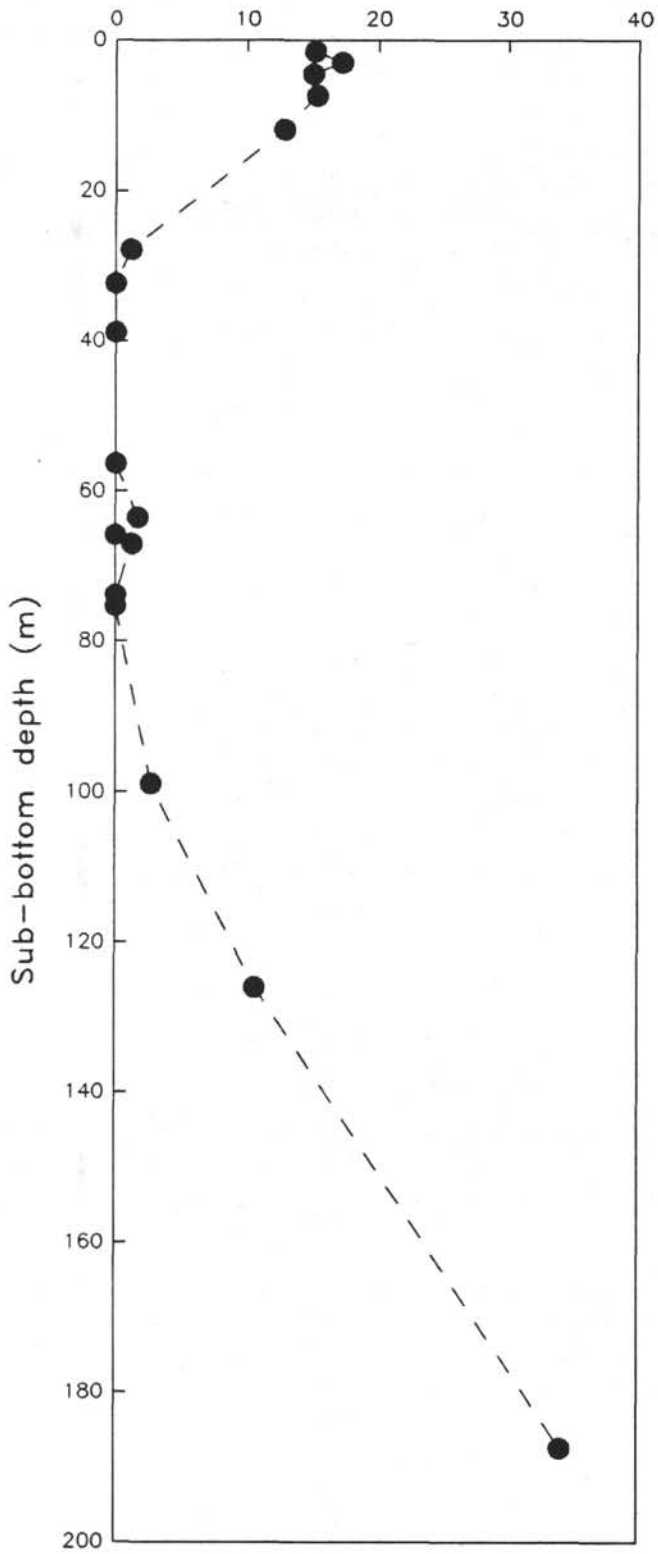


688A-15X-7 (141 mbsf)



Sulfate (mmol/L)

Methane ($\mu\text{L/L}$)



Leg 112
Operations Report
page 1

OPERATIONS REPORT

The ODP Operations Superintendent aboard JOIDES Resolution for Leg 112 of the Ocean Drilling Program was Lamar Hayes. Other operations and engineering personnel aboard JOIDES Resolution for Leg 112 were:

Wireline Coring Engineer

R. J. Klein
B.P. Research Centre
Sunbury-on-Thames
Middlesex TW16 7ln
England

Schlumberger Engineer

Lee Geiser
Schlumberger Houston
8460 Gulf Expressway
Houston, TX 77023

CALLAO PORT CALL

Leg 112 officially began at 0645 hours on 20 October, 1986, at anchorage outside the port of Callao, Peru. Once the pilot was on board JOIDES Resolution moved dockside, the first line being passed at 1030 hours. The port call was extended by four days to allow the ship's steering equipment to be completely replaced with a dual pump system that provides the ship with a redundant steering capability.

Soon after arrival in port, freight bound for TAMU and Sedco was offloaded. A total of 308,700 gallons of fuel, 4,000 sacks of barite, 688 short tons of drill water and 420 short tons of potable water were loaded, besides the oncoming surface and air freight. The scientific and technical crew changes were completed.

Thorough equipment inspections were carried out on the heave compensator, the load handling gear, the top drive, the drill pipe torque wrench and the bottom hole assembly (BHA).

CALLAO TO SITE 679

The last line was retrieved at 1515 hours on 30 October and initial steering tests were performed at anchorage outside the port. Final steering tests were conducted while underway, and at 2230 hours the ABS representative and Sedco personnel on board for the steering trials were transferred to a rendezvous vessel.

On the approach to Site 679 the seismic equipment was streamed for the pre-site survey and a spar buoy WAS jettisoned at the site location at 0830 hours on 31 October. On return to the spar buoy, a beacon was lowered on a taut wire that enabled beacon retrieval at the end of the site. The beacon featured a wide-angle capability essential for the shallow water dynamic positioning requirements of many of the Leg 112 holes.

HOLE 679A

The BHA consisted of an 11-7/16" C-4 RBI bit, a mechanical bit release (MBR), a seal bore drill collar assembly, a monel drill collar, five 8-1/4" drill collars and one 7-1/4" drill collar. After running the BHA to the mudline (434 m PDR depth) two APC cores were attempted unsuccessfully. After the second attempt, the upper core barrel section came up severely bent. It was discovered that the taut wire tension had changed and the ship had been dragging the beacon anchor along the seabed. The ship's drift could not therefore have been detected by the dynamic positioning (DP) system. The global positioning system (GPS) revealed that the ship had moved 0.85 miles east of the original position. To verify the BHA's integrity a third mudline APC was shot at the new location. Recovery of 7 m of core demonstrated that the BHA was still operational. The BHA was raised above the mudline and the ship re-positioned.

HOLE 679B

At the original location, the beacon was again lowered on a taut wire. The mudline was established at 461 m using both the BHA and the PDR, and

APC coring proceeded fast and furiously. Within eight hours, thirteen cores had been taken with an average recovery approaching 100%. The hole was terminated after the thirteenth core when a full stroke had not been obtained on the last three cores. No measurable quantities of gas were detected although the odor of hydrogen sulfide was readily discernable. The hole was abandoned with seawater.

HOLE 679C

This hole was spudded with a mudline APC core after offsetting the ship 16 m southeast of the previous hole. Excellent average core recovery in excess of 90% was maintained for the eight APC cores taken to a total depth of 385 m (75.5 mbsf). No measurable levels of gas were encountered and the hole was abandoned with seawater.

HOLE 679D

The hole was spudded 16 m southeast of Hole 679C. Heat flow and core orientation measurements were made on APC Cores 679D-6H and 679D-7H. An average of 90% recovery continued, for the 12 APC cores recovered. XCB core recovery between 540.7 m and 706.7 m (179-245 mbsf) was lower, and in an attempt to increase recovery an APC core was shot. On withdrawal the barrel parted at a mechanical failure of the core barrel box, ending the hole.

HOLE 679E

After offsetting the vessel 16 m southeast, the BHA was washed and drilled down using a center bit to a depth of 707 m (245.3 mbsf), and XCB coring commenced. Recovery averaged a little over 30%. In core 679E-12X (808.5-818 m; 346.8-356.3 mbsf) a half-inch thick silt stringer displaying petroleum fluorescence was discovered. Coring operations were ceased immediately at a total depth of 821 m (359.3 mbsf).

After termination of coring operations, the BHA was run back to bottom and the bit released for logging. The BHA was raised to the mudline and a sonic/dual induction-SFL/gamma ray/caliper (LSS-DIT-GR-CAL) logging suite was run in the open hole to refusal at 802 m (340.3 mbsf). The second logging run of gamma ray spectrometer/aluminum clay/natural gamma ray/gravitational pull intensity/telemetry cartridge tools (GST-ACT-NGT-GPIT-AMS) was complicated by downhole calibration problems with the GST, requiring an extra logging trip to replace the tool. Logging was finished after the third suite of litho-density/natural gamma/gravitational pull intensity/telemetry cartridge tools (LDT-NGT-GPIT-AMS) was run. The hole depth was reduced to 768 m (306.3 mbsf) by caving/bridging.

After rigging down the logging equipment, the drillpipe was run into the hole and the top of fill was tagged at 793 m (331.3 mbsf). The hole was circulated clean and a balanced 30-m-thick cement plug was set.

SITE 679 TO SITE 680

After the drillstring was pulled out of Hole 679E and the beacon was retrieved on the taut wire, the vessel got underway for Site 680 at 0400

hours on 5 November. The ship steamed at approximately 6 knots on approach to Site 680 for the site survey and a free-fall beacon was deployed. DP tests were conducted to fine-tune the system in preparation for the upcoming very shallow water sites.

HOLE 680A

The BHA was run to the mudline during the latter stages of the DP tests. The BHA consisted of an 11-7/16" bit, a long bit sub, a seal bore drill collar assembly, four 8-1/4" drill collars and one 7-1/4" drill collar. APC coring commenced at 1200 hours on 5 November and proceeded at an unheard-of rate: the first five cores were on deck within an hour.

After Core 680A-10H (365.3 m depth; 93.8 mbsf), a pore water sample was taken by free-falling a modified APC barrel into the sediments at the bottom of the hole. The modified barrel incorporated a spacer below the landing sub to de-couple the barrel from drillstring motion, allowing successful recovery of a pore water sample at in situ pressure. The sampler was left undisturbed in the sediments for a total of 40 minutes.

On attempting to retrieve Core 680A-11H, the core barrel box failed again, ending Hole 680A. A weakness in the threaded part of the barrel box was exacerbated by the shallow water depth.

SITE 680B

The hole was spudded with a mudline APC core after offsetting the vessel 8 m. Conventional APC coring proceeded for the first two cores. On the third and fourth core the Von Herzen heat flow shoe was added. For the heat flow measurements the APC barrel was left buried in the sediments below the bit for approximately 10 minutes to allow the shoe temperature to equilibrate. After Core 680B-7H the pore water sampler was run on an XCB barrel modified to de-couple the barrel from the drillstring. Forty minutes were allowed to elapse prior to retrieving the sampler. APC coring was then resumed until Core 680B-9H (364.5 m depth, 92.0 mbsf), when XCB coring began. Excellent average APC core recovery in excess of 100% was recorded, but XCB recovery was between 0 and 16%, averaging less than 5%. Owing to the poor XCB recovery between 364.5 m and 468 m (92-195.5 mbsf), it was decided to abandon Hole 680B with weighted mud as a precautionary measure.

HOLE 680C

This hole was spudded 8 m from the previous hole, and four APC cores were recovered between the mudline at 272.2 m and total depth of 306.5 m (0-34.3 mbsf). In situ heat flow measurements were taken prior to recovery of the last two cores. While retrieving Core 680C-4H the sandline parted at the rope socket and fishing attempts failed, requiring that the pipe be tripped out of the hole. By 2200 hours on 6 November, the ship was underway at 6 knots for Site 681.

SITE 680 TO SITE 681

Site 681 was approached approximately 2.5 hours later and a spar buoy was deployed. Coring was postponed until a Satnav fix was received, pinpointing the vessel 1.6 miles off location. By 0700 hours the correct site location had been reached in DP mode and a taut-wire beacon lowered.

HOLE 681A

The first APC core established the mudline at 161.3 m depth. This was the shallowest water depth JOIDES Resolution had ever cored in. Rapid APC coring ensued, and the first seven cores were on deck within two hours. The seventh core was followed by the pore water sampler. Another pore water sample was taken after the eleventh APC core. The APC recovery to a depth of 272.3 m (120.5 mbsf) averaged 85%. XCB recovery for the remainder of the hole (348.3 m; 187.0 mbsf) averaged 22%. After taking a pore water sample in the sediments at the bottom of the hole, the hole was displaced with weighted mud in view of the uncertainty associated with the extremely low recovery obtained for the last four XCB cores (less than 5%).

HOLE 681B

Operationally Hole 681B was largely a repeat of Hole 681A. APC coring reached a depth of 248.4 m (86.5 mbsf), followed by XCB coring to 305.4 m (143.5 mbsf). Pore water samples were taken at 224.8 and 286.4 m (62.9 and 124.5 mbsf). APC and XCB recovery on this hole averaged 83% and 45%, respectively.

HOLE 681C

The ship was offset 8 m and ten APC cores were taken between the mudline at 161.9 m and 253.8 m (91.4 mbsf), with a recovery rate of 90%.

SITE 681 TO SITE 682

Site 681 was departed at 1800 hours on 7 November. Seven hours later the geophysical equipment was streamed for the site approach. A beacon was deployed on the first pass and the ship maneuvered into position.

HOLE 682

The BHA consisted of an 11-7/16" type C4 bit, a seal bore drill collar assembly, four 8-1/4" drill collars and one 7-1/4" drill collar. The mudline was established at 3801.6 m. APC recovery averaged in excess of 90%. Thick-wall liners were used, requiring that the cores be cut in a smaller diameter.

XCB recovery averaged approximately 20%. At 4096 m (295 mbsf) a noticeable decrease in penetration rate was accompanied by a significant increase in core recovery (approximately 40% recovery from 4096.4 to 4169.5 m). Below 4169.5 m (368.2 mbsf) recovery again dropped off, averaging less than 20% for the remainder of the hole. Two pore water samples were taken at depths of 3224.4 m and 3328.9 m (142.8 and 247.3 mbsf).

Deteriorating hole conditions were noted after cutting Core 682A-42X. After cutting Core 682A-48X to a depth of 4238 m (436.7 mbsf) the pipe stuck at 4230 m (1148.4 mbsf). After three hours, a drill pipe severing tool was run into the hole and detonated. The pipe was severed but still required 20,000 lbs overpull to withdraw it, indicating that the packed off section extended above the severing charge depth. The hole was displaced with heavy mud and abandoned.

SITE 682 TO SITE 683

Site 682 was departed at 1715 hours on 14 November. Fourteen hours later a recallable beacon was dropped at Site 683. A second beacon was deployed because of a weak signal from the first, which was recalled.

HOLE 683A

The new BHA consisted of an 11-7/16" bit, a MBR, a seal bore drill collar assembly, five 8-1/4" drill collars, a mechanical jar, two 8-1/4" drill collars and one 7-1/4" drill collar. An APC core established the mudline at 3086.6 m. A heat flow shoe was added for Core 683A-5H. APC core recovery averaged 72%.

After 9 APC cores, XCB coring began at 3164.8 m (78.2 mbsf). Penetration rates while XCB coring were variable but generally good, and core recovery was also variable. The mean XCB recovery was 43%, and the overall average for the hole was 52%.

Although regular attempts were made to improve hole conditions, after cutting Core 683A-44X to a depth of 3496.3 m (409.7 mbsf), the hole deteriorated rapidly. To avoid a stuck BHA, the hole was displaced with mud and the bit pulled above the mudline after cutting Core 683A-45X to a total depth of 3505.8 m (419.2 mbsf). The ship was then offset 300 m east, the barrel containing Core 683A-45X retrieved, and a wash barrel with a center bit was dropped.

HOLE 683B

The location of Hole 683B was selected to avoid penetration of the unstable slumped sediments encountered in Hole 683A. XCB coring commenced after drilling with the center bit to a depth of 3479 m (412 mbsf). Hole conditions remained good to 3545.5 m (469 mbsf), after which conditions worsened. The hole was deemed too unstable to log and was displaced with heavy mud prior to pulling the drillstring. The total depth of the hole was 3564.5 m (488 mbsf).

SITE 683 TO SITE 684

The ship left Site 683 at 1800 hours on 21 November, slowing to 6 knots for the approach to Site 684. The geophysical gear was streamed and the survey results used to identify a mud lens of particular scientific interest prior to selecting the site. A spar buoy was deployed at 2300 hours and a taut-wire beacon was lowered. At 0130 hours on 22 November, after running the BHA to 200 m, GPS indicated the ship to be 1.5 miles from the desired site location. The drillstring was pulled to within one stand

of the BHA and ship was re-positioned at the correct location using the thrusters.

HOLE 684A

A six drill-collar APC/XCB BHA was made up with a long bit sub. The mudline was established at 437.7 m. Full strokes of the APC were achieved for the first four cores, followed by four partial APC strokes. Sediment heat flow was measured prior to retrieving cores 684A-4H and 684A-6H. APC core recovery averaged 99%. The pore water sampler was deployed prior to XCB coring and was retrieved with the entire lower section of the core barrel bent, probably by deflection off a boulder or a hard sedimentary horizon.

Coring operations were suspended while the supply ship M/V Rios transferred cargo and personnel. An hour later operations were resumed with the XCB. Hole 684A was terminated prematurely at 573.8 m (136.1 mbsf) because XCB core recovery was averaging 5%. After raising the BHA to clear the mudline, the ship was offset 8 m west and a new hole spudded.

HOLE 684B

Five APC cores followed by one XCB core were taken for a total penetration of 55 m below the 438.5-m mudline. Although APC recovery averaged 80%, no core was recovered with the XCB. The mudline was cleared and the ship offset 8 m south.

HOLE 684C

The mudline was established at 438.2 m and five APC cores cut with an average recovery in excess of 100%. Hole 684C was deepened with the XCB to a total depth of 553.2 m (115.0 mbsf). XCB core recovery averaged 20%, a welcomed improvement over the previous two holes at this site. One possible explanation for the improved recovery may be a combination core catcher used in this hole.

SITE 684 TO SITE 685

The transit from Site 684 to Site 685 took four and a half hours. Geophysical data were collected approaching Site 685. The beacon was dropped at 1315 hours on 22 November.

HOLE 685

A BHA was made up consisting of an 11-7/16" bit, a MBR, a seal bore drill collar assembly, five 8-1/4" drill collars, one mechanical jar, two 8-1/4" drill collars and one 7-1/4" drill collar. One APC water core was shot before establishing the mudline at 5093.4 m. APC recovery averaged in excess of 100%.

XCB coring began with Core 685A-5X at a depth of 5126 m (32.6 mbsf). To a depth of 5259 m (165.6 mbsf) core recovery was at least 40% and on six cores it exceeded 100%. Between 5259 m and 5450.5 m (165.6-357.1 mbsf) core recovery was highly variable, ranging from 0% (Core 685A-24X) to 135%

(Core 685A-18X). Between 5450.5 m and the total depth of 5562.0 m (357.1-468.6 mbsf) core recovery never exceeded 40%.

The great variability in core recovery was most likely because of the live gas hydrates encountered in many of the cores between 5164 m and 5450.5 m (70.6-357.1 mbsf). On removing the core catcher, the core liner frequently shot out of the barrel, driven by gas pressure within the core. Where recovery in excess of 100% was recorded, this was invariably due to expansion of gas hydrates forming voids in the cores.

Below a depth of 5306.5 m (213.1 mbsf) a sharp decrease in penetration rate was apparent. After retrieving Core 685A-40X to a depth of 5460 m (366.6 mbsf) rotation was not possible and the bit had to be pulled to 5444 m (350.6 mbsf) before circulation could be regained. The drillstring again stuck while retrieving Core 685A-50X and while making a connection after cutting Core 685A-51X. The bit was released for logging after pulling the drillstring to 5166 m (82.1 mbsf).

Three suites of logs were run in Hole 685. A bridge at 5380 m limited log penetration to 286.6 mbsf. The first suite was a dual induction-SFL/gamma ray/caliper/sonic combination (DIT/GR/CAL/SLT). The second logging suite consisted of a gamma ray spectrometer/aluminium clay tool/compensated neutron/natural gamma ray/gravitational pull intensity tool/auxiliary measurement tool/telemetry cartridge (GST/ACT/CNTG/NGT/GPIT/CCCB/AMS). The final logging run comprised the litho-density/compensated neutron/natural gamma ray/auxiliary measurement services (LDT/CNTG/NGT). The logging tools were rigged down by 2315 hours on 29 November. The drillstring was run to 5338 m (244.6 mbsf) and the hole displaced with mud.

SITE 685 TO SITE 686

By 0930 hours on 30 November, the ship had begun the 30-hour transit to Site 686. While underway, a used R&I C-3 XCB bit was extensively modified in an attempt to improve bit cleaning design deficiencies identified while performing flow tests earlier in the leg.

On the approach to Site 686 the ship slowed to below 6 knots and the seismic gear was streamed. A shallow water beacon was dropped at 1730 hours on 1 December. A weak signal from the beacon allowed the ship to drift 350 ft off location. A taut-wire beacon was deployed immediately.

HOLE 686A

A BHA consisting of the modified 11-7/16" bit, a seal bore drill collar assembly, four 8-1/4" drill collars and one 7-1/4" drill collar was made up and run to the seafloor. The mudline was established at 458.7 m with an APC core. Seven more APC cores to a depth of 523.4 m (64.7 mbsf) were recovered before picking up the XCB. Heat flow measurements were taken on Cores 686A-4H and 686A-6H. APC recovery averaged 89%.

The hole was deepened to a total depth of 664.4 m (205.7 mbsf) with the XCB. XCB recovery averaged 88%. In addition, no significant reduction in penetration rate was observed as the hole was deepened. This suggested that the bit modifications were effective in improving cone cleaning and

hence bit performance. It is also possible that the improved penetration rate may have contributed to the increase in core recovery.

Pore water samples were taken after Cores 686A-13X and 686A-21X. The hole was displaced with mud prior to clearing the mudline with the BHA and spudding Hole 686B 8 m south.

HOLE 686B

The mudline was established at 458.3 m. APC recovery averaged 97%. XCB coring began with the sixth core and averaged 70%. The rapid penetration rate obtained while coring Hole 686A continued in this hole. The final hole total depth was 761.3 m (303.0 mbsf). The hole was displaced with mud before pulling out.

SITE 686 TO SITE 687

The ship was underway from Site 686 to Site 687 at 0300 hours on 3 December. On arrival at Site 687 at 0700 hours, the taut-wire beacon from the previous site was lowered and the vessel positioned in DP mode.

HOLE 687A

This hole was spudded with an APC mudline core at 316.3 m. Five more APC cores were taken including two with heat flow measurements (Cores 687A-4H and 687A-6H). Excellent APC recovery in excess of 100% was obtained.

XCB coring deepened the hole from 371.3 m (64.5 mbsf) to a total depth of 371.3 m (207.0 mbsf). XCB core recovery averaged 34%. The pore water sampler was deployed once, after Core 687A-18X. On reaching total depth, the BHA was raised above the mudline and the ship offset 8 m south.

HOLE 687B

The mudline was established at 315.6 m, and eleven APC cores were recovered to a depth of 406.4 m (90.8 mbsf). The hole was deepened to a total depth of 510.9 m (195.3 mbsf) using the XCB. XCB recovery averaged 19%.

SITE 687 TO SITE 688

The ship was underway from Site 687 at 1200 hours on 4 December. The seismic gear was streamed approaching Site 688 and the beacon was dropped at 1715 hours. By 1900 hours the ship was in DP mode and the drillstring was on its way down.

HOLE 688A

The BHA selected for this hole consisted of an 11-7/16" bit, MBR, seal bore drill collar assembly, five 8-1/4" collars, one jar, two 8-1/4" drill collars and one 7-1/4" drill collar. An APC core established mudline at 3828.5 m. The heat flow shoe was deployed on Core 688A-4H. Excellent average APC recovery in excess of 100% was achieved.

The XCB was used after Core 688A-7H (3893.8 m; 65.3 mbsf) to a total depth of 4178.8 m (350.3 mbsf). The pore water sampler was deployed after Cores 688A-5H, 688A-17X, 688A-27X and 688A-37X. After Core 688A-37X the pore water sampler was lost in the hole when the core barrel box threads once again failed. Attempts to recover the sampler were unsuccessful. The hole was filled with mud and the BHA pulled to the mudline to spud Hole 688B.

XCB recovery averaged 62%. Live gas hydrates were recovered in Core 688A-15X, while Cores 688A-11X, 688A-14X and 688A-16X exhibited spectacular gas expansion.

HOLE 688B

After clearing the mudline, the ship was offset 30 m west and Hole 688B was spudded with a center bit to drill down to 4178.8 m (350.3 mbsf). Five unsuccessful attempts were made to retrieve the center bit. The hole was filled with mud and the drillstring tripped out of the hole. The center bit/barrel assembly was found to have not latched in correctly because a ten-inch section of the pore water sampler was wedged in the guide ring and float valve, the flapper having been broken. The center bit/barrel assembly was presumed to have been sanded in.

HOLE 688C

A rotary coring BHA was made up consisting of a 9-7/8" bit, hydraulic bit release (HBR), outer barrel assembly, five 8-1/4" drill collars, one jar, two 8-1/4" drill collars and one 7-1/4" drill collar. Hole 688C was spudded in 3836.3 m of water and drilled with a wash barrel/center bit to 4178 m (341.7 mbsf). An RCB core was cut to 4188.3 m (359.8 mbsf) but the barrel could not be retrieved, requiring that the hole be displaced with mud and the drill string tripped out for repair.

HOLE 688D

The BHA was run back to the seafloor at 3836 m and drilled to 4010 m (174 mbsf) with the wash barrel/center bit in place. This hole had retrieval problems similar to those at Hole 688C, requiring that the hole be displaced with mud and the drillstring tripped out of the hole.

HOLE 688E

Extensive precautions were taken to prevent recurrence of the retrieval problems. The rotary core barrel BHA was made up and run to the seafloor at 3836 m. The hole was drilled with the wash barrel/center bit to 4186.3 m (355.5 mbsf) and fourteen rotary cores were taken. RCB recovery in Hole 688E averaged 35%. A deviation survey on Core 688E-31R (4476.8 m; 640.5 mbsf) indicated the hole to be within 1° of vertical.

RCB coring continued until a stuck core barrel, poor hole conditions and time constraints caused the hole to be terminated at 4615.3 m (779 mbsf). Logging was prevented by the stuck core barrel. The hole was displaced with mud and abandoned.

SITE 688 TO CALLAO

The beacon was recalled and the ship was underway for Callao at 1730 hours on 19 December. The ship moved to berth on 19 December, the first line being cast at 0630 hours.

CALLAO PORT CALL

A brief port call was made in Callao during which the scientific staff disembarked and some of the ODP staff were relieved. The ship was refueled and after 30.5 hours in port left to transit to Valparaiso, Chile, on 20 December.

TRANSIT TO VALPARAISO

Eighteen ODP personnel were aboard for the transit. The technical staff remodeled the co-chiefs' staterooms and the new co-chief scientists' office on the ship's bridge deck. An inventory was made of all government-funded equipment aboard ship. Geophysical data were collected with the magnetometer and water guns. The transit ended in Valparaiso at 0900 on Christmas day, 1986.

OCEAN DRILLING PROGRAM
OPERATIONS RESUME
LEG 112

Total Days		66
Total Days in Port		11.6
Total Days Under Way		9.6
Total Days on Site		44.8
	Trip Time	7.9
	Coring Time	28.3
	Drilling Time	3.0
	Logging/Downhole Science Time	1.9
	Mechanical Repair Time (contractor)	.3
	Stuck Pipe & Hole Trouble	.3
	Other	3.1
Total Distance Traveled (nautical miles)		2243
Average Speed (knots)		9.4
Number of Sites		10
Number of Holes		27
Number of Cores		498
Total Meters Cored (m)		4701.3
Total Core Recovery (m)		2578
Percent Core Recovered		54.7
Total Interval Drilled (m)		2053
Total Penetration (m)		6754
Maximum Penetration (m)		779
Minimum Penetration (m)		7
Maximum Water Depth (m from drilling datum)		5093
Minimum Water Depth (m from drilling datum)		161
Average Water Depth (m)		1790

OCEAN DRILLING PROGRAM
 SITE SUMMARY
 LEG 112

HOLE	LATITUDE	LONGITUDE	DEPTH METERS	NUMBER OF CORES	METERS CORED	METERS RECOVERED	PERCENT RECOVERED	METERS DRILLED	TOTAL PENET.	TIME ON HOLE	TIME ON SITE
679A	11° 03.52 S	78° 15.92 W	434	1	7	7	100	---	7	8.75	---
679B	11° 03.80 S	78° 16.34 W	461	13	107.2	103	96.1	---	107.2	10.50	---
679C	11° 03.81 S	78° 16.33 W	460.5	8	75.5	69.7	92.4	---	75.5	5.75	---
679D	11° 03.828S	78° 16.39 W	461.7	27	245.4	115.8	47.1	---	245.4	24.75	---
679E	11° 03.78 S	78° 16.34 W	461.7	13	114.3	36.3	31.8	245	359.3	62.50	112.25
680A	11° 83.06 S	78° 04.67 W	271.5	10	93.8	81.2	87	---	93.8	13.50	---
680B	11° 03.90 S	78° 04.67 W	272.5	22	195.5	98.4	50.4	---	195.5	18.00	---
680C	11° 03.925S	78° 04.6 W	272.2	4	34.3	35	102	---	34.3	7.50	39.00
681A	10° 58.60 S	77° 57.46 W	161.3	20	187	112.3	60	---	187	22.75	---
681B	10° 58.6 S	77° 57.46 W	---	---	143.5	97.3	67.8	---	143.5	13.25	---
681C	10° 58.6 S	77° 57.46 W	161.9	10	91.4	90.3	98.7	---	91.4	4.75	40.75
682	11° 15.99 S	79° 08.73 W	3801.3	48	436.7	127.4	29.1	---	436.7	143.00	143.00
683A	9° 01.69 S	82° 24.40 W	3086.6	45	419.2	219.1	52.2	---	419.2	80.25	---
683B	9° 01.59 S	80° 24.26 W	3076.5	9	85.5	30.6	35.7	402.5	488.0	50.50	130.75
684A	8° 59.49 S	79° 57.35 W	437.7	15	136.1	72.5	53.2	---	136.1	16.25	---
684B	8° 59.49 S	79° 57.35 W	438.5	6	55	37.2	67.6	---	55	4.25	---
684C	8° 59.49 S	79° 57.35 W	438.2	13	115	56.2	48.8	---	115	12.25	32.75
685A	9° 06.78 S	8° 35.01 W	5093.4	51	468.6	278.6	59.4	---	468.6	188.25	188.25
686A	13° 28.81 S	78° 53.49 W	458.7	23	205.7	181.7	88.3	---	205.7	17.25	---
686B	13° 28.81 S	76° 53.49 W	458.3	32	303	225.5	74.4	---	303	13.00	30.25
687A	12° 51.78 S	78° 59.43 W	316.3	22	207	108.3	52.3	---	207	11.50	---
687B	12° 51.78 S	78° 59.43 W	316.3	22	195.3	87.4	44.7	---	195.3	11.75	23.25
688A	11° 32.26 S	78° 56.57 W	3828.5	37	350.3	245	70	---	350.3	57.00	---
688B	11° 32.26 S	78° 56.57 W	3828.5	---	---	---	---	360	360	25.00	---
688C	11° 32.26 S	78° 56.57 W	3836.3	1	9.5	1.2	12	350.3	359.8	38.50	---
688D	11° 32.26 S	78° 56.57 W	3836.3	---	---	---	---	345	345	30.00	---
688E	11° 32.26 S	78° 56.65 W	3836.3	46	429	152	35.4	350	---	185.50	336
TOTALS				498	4710.6	2578	54.7	2053	6763.6		1076.25

OCEAN DRILLING PROGRAM
 BEACON SUMMARY
 LEG 112

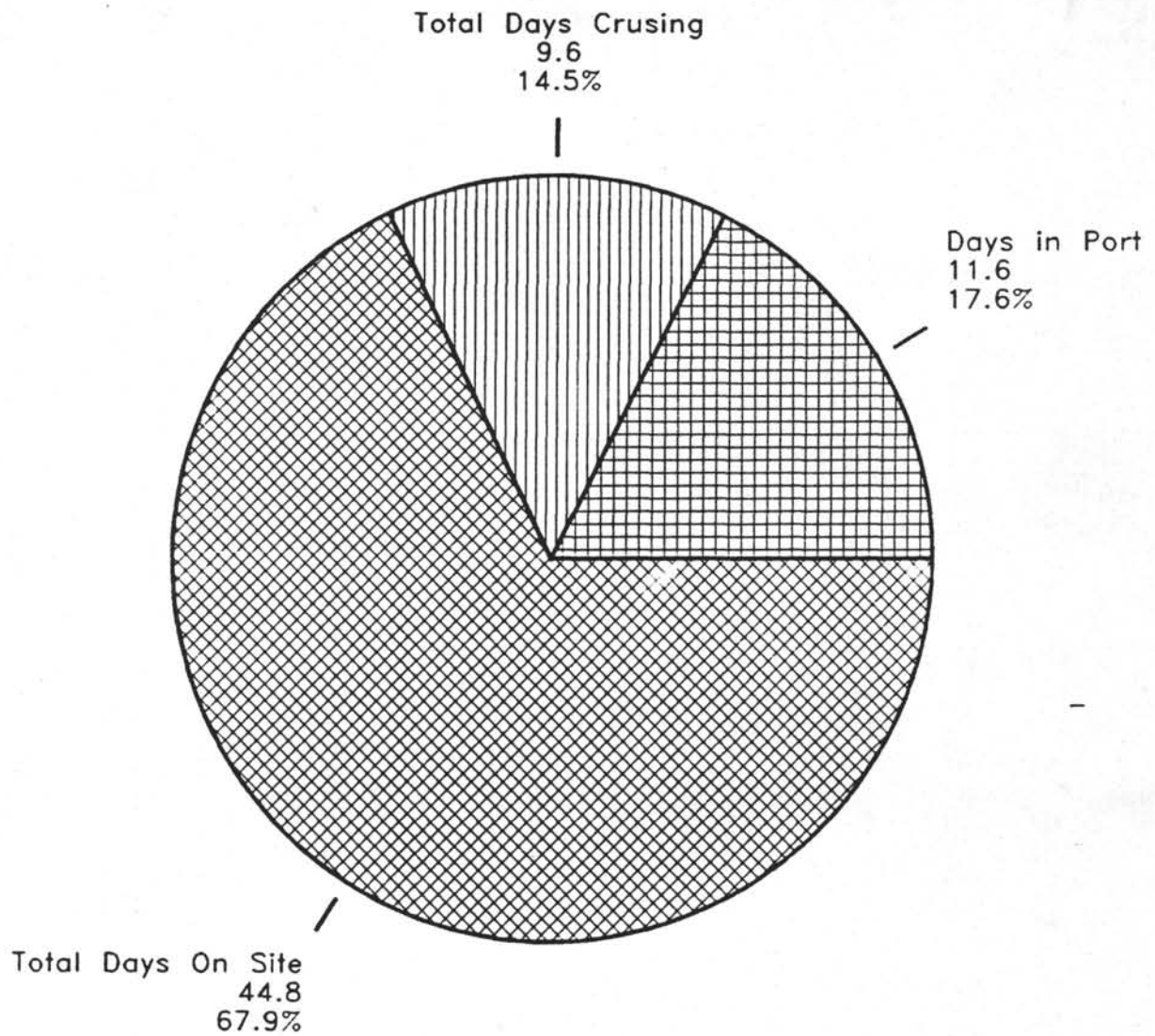
<u>SITE</u>	<u>MAKE</u>	<u>FREQ.</u> <u>KHZ</u>	<u>SERIAL</u> <u>NUMBER</u>	<u>SITE</u> <u>TIME</u>	<u>WATER</u> <u>DEPTH</u> <u>METERS</u>	<u>REMARKS</u>
679	DATASONICS	15	315	112.25	460	RAN ON TAUT WIRE.
680	DATASONICS	14	314	39.00	264	GOOD SIGNAL.
681	DATASONICS	15	315	40.75	161	RAN ON TAUT WIRE. RERUN FROM SITE 679.
682	DATASONICS	16.5	352	143.00	3800	GOOD SIGNAL.
683	DATASONICS	14.5	306	126.75	3083	RECALLABLE BEACON. WEAK SIGNAL, RECALLED BEACON.
683	DATASONICS	16.5	291	4.00	3083	WOULD MISS 2-3 PULSES IN A ROW. NOT A GOOD BEACON.
684	DATASONICS	15	315	32.00	483	RAN ON TAUT WIRE. RERUN FROM SITE 681. GOOD BEACON.
685	DATASONICS	15.5	305	188.25	5093	GOOD SIGNAL.
686	DATASONICS	16	316	3.25	455	BEACON FAILED AFTER 3-1/4 HRS. RAN T/W BACK UP.
686	DATASONICS	15	315	27.00	455	RAN ON TAUT WIRE. USED LAST ON SITE 684.
687	DATASONICS	15	315	23.25	316	RAN ON TAUT WIRE. USED LAST ON SITE 686.
688	DATASONICS	14.5	306	336.00	3836	RECOVERABLE; GOOD SIGNAL, BEACON WAS RECOVERED.

OCEAN DRILLING PROGRAM
BIT SUMMARY
LEG 112

HOLE	MFG	SIZE	TYPE	SERIAL NUMBER	METERS CORED	METERS DRILLED	TOTAL PENET	CUMULATIVE METERS	HOURS THIS HOLE	TOTAL HOURS	CONDITION	REMARKS
679A	MSDS	11-7/16	C-4	RR	7	---	---	7	---	39-3/4	N/A	---
679B	MSDS	11-7/16	C-4	RR	107.2	---	107.2	114.2	---	39-3/4	N/A	---
679C	MSDS	11-7/16	C-4	RR	75.5	---	75.5	189.7	---	39-3/4	N/A	---
679D	MSDS	11-7/16	C-4	RR	245.4	---	245.4	435.1	2-1/2	42-1/4	N/A	---
679E	MSDS	11-7/16	C-4	RR	114	245	359	794.1	10	52-1/4	N/A	RELEASED TO LOG.
680A	R&I	11-7/16	C-3	680	93.8	---	93.8	93.8	---	---	---	---
680B	R&I	11-7/16	C-3	680	195	---	195	288.8	2-1/2	2-1/2	---	---
680C	R&I	11-7/16	C-3	680	34.3	---	34.3	323.1	---	2-1/2	B1-T1-G	---
681A	R&I	11-7/16	C-3	680	187	---	187	510	1-1/2	4	---	---
681B	R&I	11-7/16	C-3	680	143.5	---	143.5	652.5	1-1/2	5-1/2	---	---
681C	R&I	11-7/16	C-3	680	91.4	---	91.4	743.9	---	5-1/2	B1-T1-G	---
682A	RBI	11-7/16	C-4	AS814	436.7	---	436.7	436.7	31	31	N/A	LOST IN HOLE.
683A	RBI	11-7/16	C-3	AV193	419.2	---	419.2	855.9	9-1/4	40-1/2	N/A	---
683B	RBI	11-7/16	C-3	AV193	85.5	402.5	488	1343.9	16-3/4	57	B2-T1-G	---
684A	RBI	11-7/16	C-3	AV193	136.1	---	136.1	1479.1	1-3/4	58-3/4	---	---
684B	RBI	11-7/16	C-3	AV193	55	---	55	1534	1-1/2	60-1/4	---	---
685	RBI	11-7/16	C-3	AV193	468.6	---	468.6	2002.6	19	79-1/4	N/A	RELEASED FOR LOGGING.
686A	R&I	11-7/16	C-3	680	205.7	---	205.7	949.6	1-3/4	7-3/4	---	MODIFIED JETS.
686B	R&I	11-7/16	C-3	680	303.0	---	303.0	1252.6	3-3/4	11-1/2	B1-T2-G	MODIFIED JETS.
687A	R&I	11-7/16	C-3	680	207.0	---	207.0	1459.6	1	12-1/2	---	MODIFIED JETS.
687B	R&I	11-7/16	C-3	680	195.3	---	195.3	1654.9	1	13-1/2	B1-T2-G	MODIFIED JETS.
688A	R&I	11-7/16	C-3	680	350.3	---	350.3	2005.2	9	22-1/2	---	MODIFIED JETS.
688B	R&I	11-7/16	C-3	680	---	360	360.0	2365.2	10	32-1/2	B2-T2-1G	MODIFIED JETS.
688C	RBI	9-7/8	C-3	AP631	9.5	350.3	359.8	359.8	9-1/2	9-1/2	NEW	4 x 16 JETS.
688D	RBI	9-7/8	C-3	AP631	---	345	345	704.8	10	19	NEW	4 x 16 JETS.
688E	RBI	9-7/8	C-3	AP631	429	350	779.0	779.0	35	54-1/2	B2-T7-1/8	4 x 16 JETS.

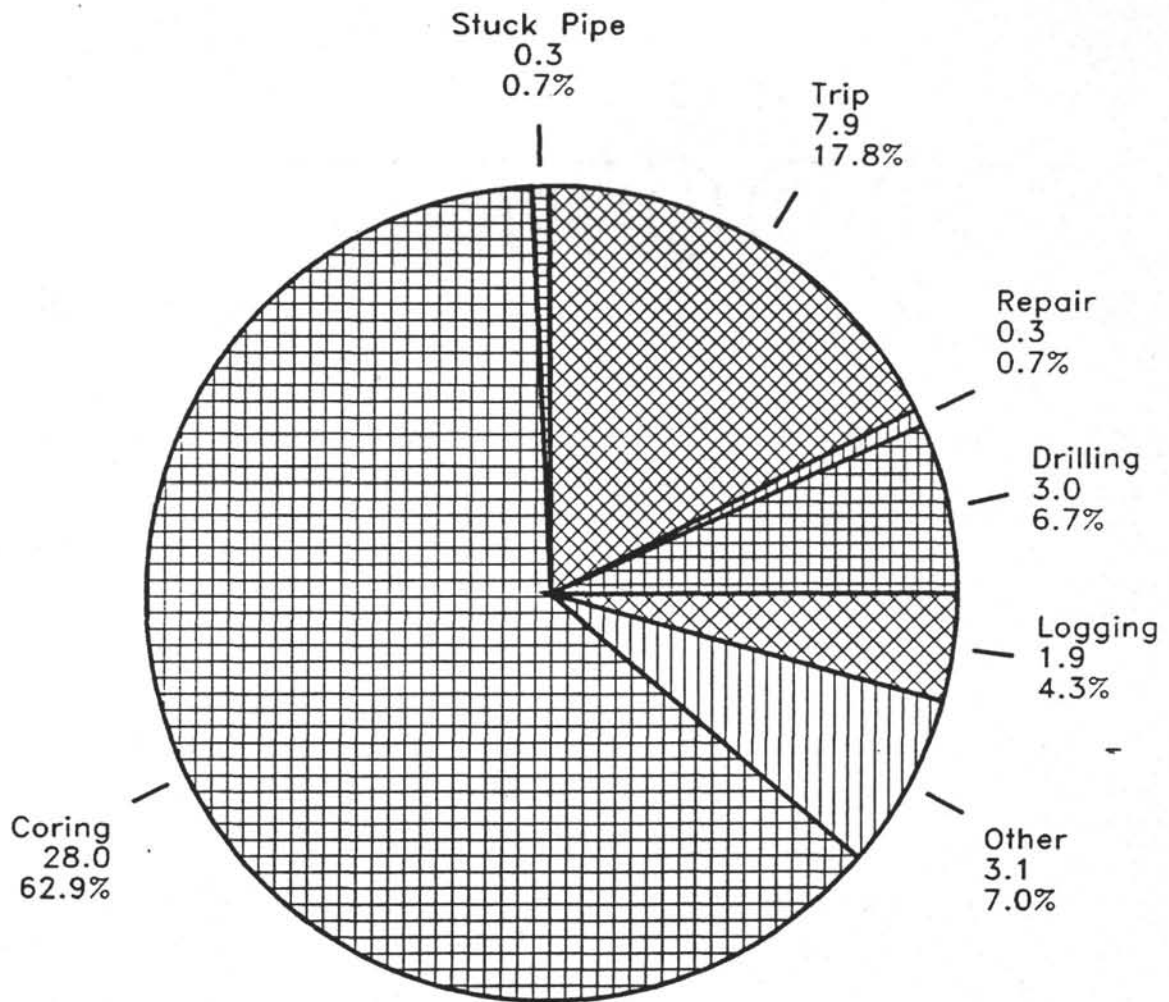
Leg 112

Duration: 66.0 Days



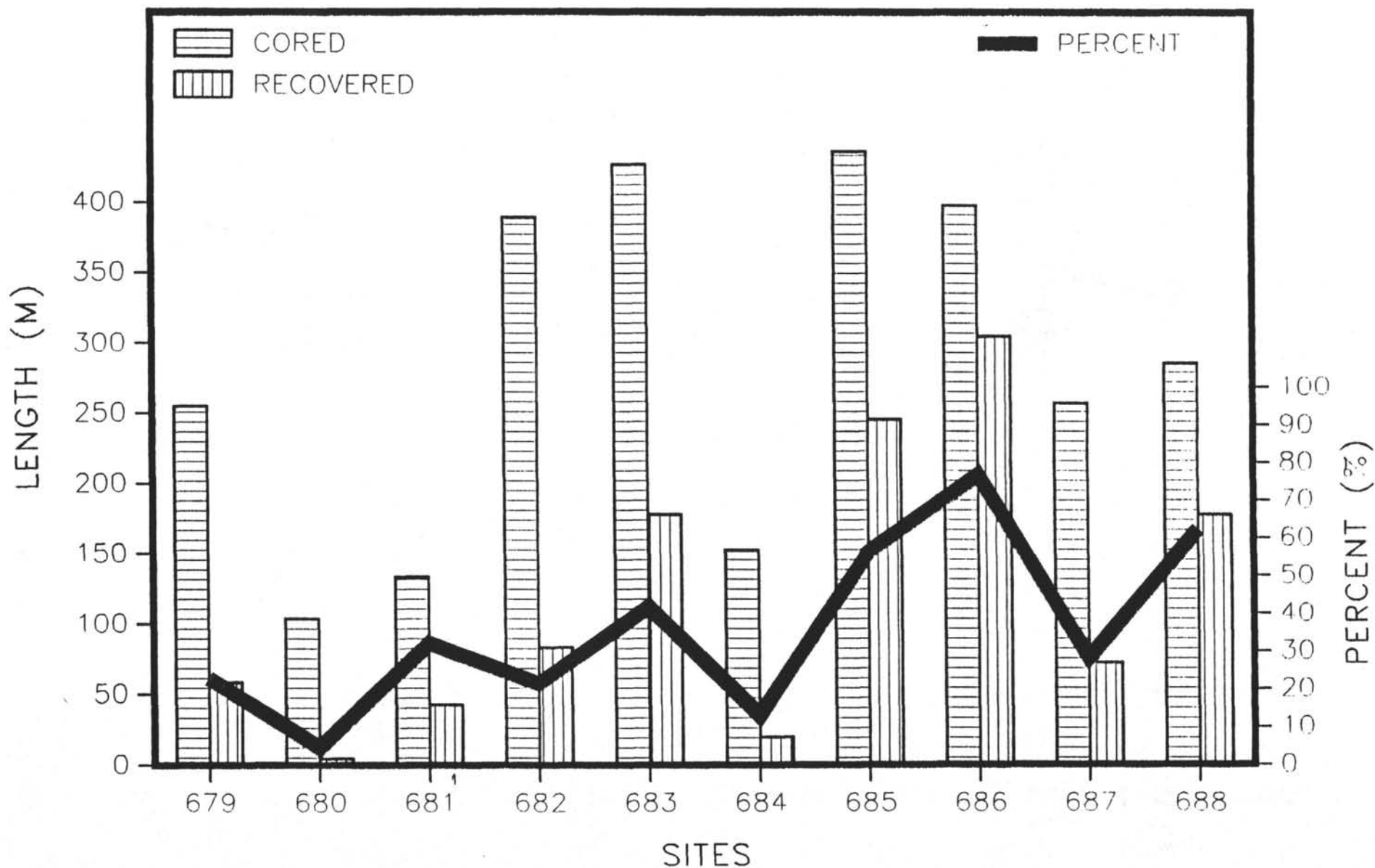
On Site Time

Total Time On Site: 44.8 Days



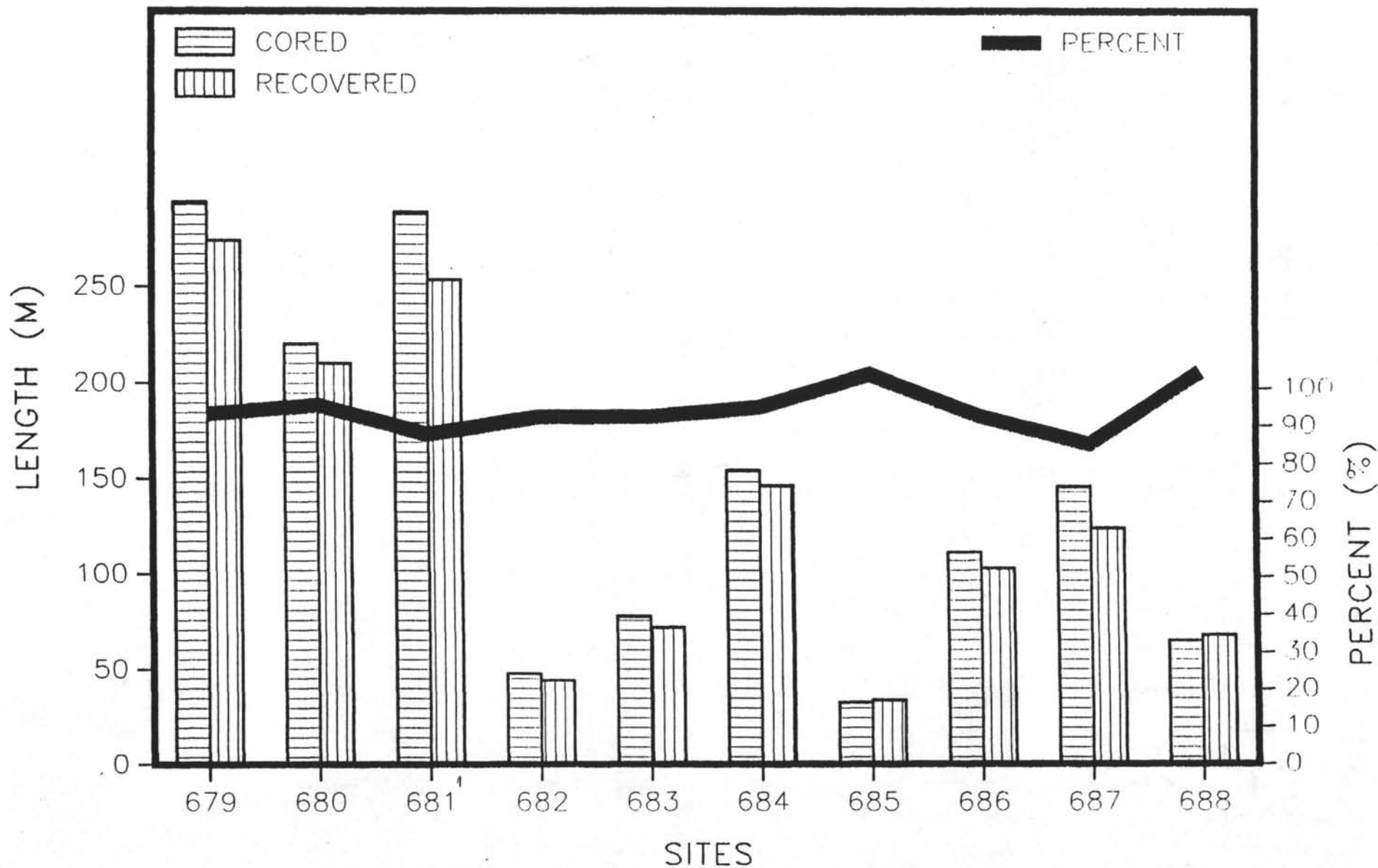
LEG 112 : XCB PERFORMANCE

MEAN RECOVERY : 41.8 %



LEG 112 : APC PERFORMANCE

MEAN RECOVERY : 92.4 %



TECHNICAL REPORT

The ODP Technical and Logistics personnel aboard JOIDES Resolution for Leg 112 of the Ocean Drilling Program were:

Laboratory Officer:	Burney Hamlin
Computer System Manager:	Daniel Bontempo
Curatorial Representative:	Paula Weiss
Senior Marine Technician:	Brad Julson
Yeoperson:	Michiko Hitchcox
Photographer:	Chris Galida
Electronics Technician:	Mike Reitmeyer
Chemistry Technician:	Matt Mefferd
Chemistry Technician:	Katie Sigler-Tauxe
X-ray Technician:	Christian Segade
Marine Technician:	Jenny Glasser
Marine Technician:	Linda Mays
Marine Technician:	Dean Merrill
Marine Technician:	Joe Powers
Marine Technician:	Kevin Rogers
Marine Technician:	Don Sims
Marine Technician:	John Tauxe

The technical staff for Leg 112 arrived in Lima, Peru late on 19 October 1986. JOIDES Resolution arrived in the port of Callao on the 20th, initially anchoring out until 0930, then coming in to dock and to clear customs. Crossover began near lunch time on 21 October and continued all day.

PORT CALL

Air and surface freight from College Station arrived at the ship promptly; the air freight on 21 October and the two 40' surface containers on 22 October. The shipments were dispersed and stored. The D-tubes to accommodate the expected high recovery for the leg were stacked high under the hatch and lashed down. Barite was loaded manually.

Leg 111's air and surface freight were off-loaded on 25 October. Heavy pieces of drilling equipment, the cryogenic magnetometer, and various other pieces for surface shipment were staged in a warehouse where technicians loaded a container assuring that the load would be balanced and as secure as possible. The frozen shipment of sediment samples, the hard rock base parts which were to be shipped break bulk, and an empty core liner box for disposal were off-loaded on 29 October.

Xerox serviced the two units aboard ship. An electronics technician recommended by the agent worked unsuccessfully on the lounge video projector. The unit was packed for airshipment to the USA for repair.

UNDERWAY

After the steering gear and auto pilot features were tested and approved on sea trials, the SEDCO engineers and ABS official departed on the Pilot boat. JOIDES Resolution departed Callao harbor near 2200 hours on 30 October for our first site, 689. The 12 and 3.5 kHz depth recorders were turned on and, once sufficient depths were reached, one water gun, a hydrophone array, and a magnetometer sensor were deployed. Two new Raytheon flat bed recorders, set up but unused last cruise, were turned on for an analog seismic record. While the ship cruised at ten knots through the night monitoring the new steering installation, the underway lab records were buried in noise despite hours of signal gains and recorder adjustments. All records cleared up when the ship slowed to six knots for a brief site survey.

Other transits were made at 12 knots with the magnetometer and depth recorders only. The seismic equipment was deployed for short six-knot site surveys with satisfactory results. The co-chiefs decided to use the 3.5-kHz depth recorder to select Site 683, a small shallow-water sediment pond. The magnetometer was not deployed on the short transit from site 684 to 685 when the MASSCOMP computer system failed. After running diagnostics and rebooting the programs the system ran normally. The transit from Site 685 to Site 686 was our longest at 32 hours.

CORE LAB

The core lab accommodated the high number of cored sections by slightly modifying the routine. One section per core was GRAPE'd on the "A" holes

and as many as possible on the "B" holes while appropriate sections adjacent to discrete in situ heat flow measurements equilibrated to room temperature. The absence of the cryogenic magnetometer, too, allowed for cores to pass through the lab faster than on earlier legs. It was unfortunate, nevertheless, as the magnetic signatures in the sediments recovered were weak, many below the noise level of the Minispin magnetometer. For the most part, lab equipment worked satisfactorily. A spare vane shear replaced our new unit which had a defective clutch.

The "richness" of the shallow cores was evident throughout the lab assembly when cores were being cut. The ultra-violet light box was kept handy throughout the leg to check suspicious areas for fluorescence. The gassy cores made the catwalk hazardous when the core cutting shoe was removed from the core barrels. Some videos were taken of the liner ejecting out of the barrel and impacting accordion style into a barrel and plywood barrier put up to shield the catwalk.

CURATORIAL REPORT

The numerous very shallow sites with multiple holes, short distances between sites, and several very special sampling programs proved hectic, but fortunately, the duration of the multiple sites was limited by depth to a couple days each. A record 99 cores in 54 hours was received by the core lab at Site 686 and 687 including the transit.

Over 2500 m of sediment was recovered, described, sampled and archived resulting in approximately 12,000 samples. Some of the shallow water samples were unusually rich in biological remains, including sponge spicules, fish and marine mammal bones, and sea shells. Parts of some seemingly living worms were recovered and preserved. Special biological samples were taken which were carefully chilled or frozen. Forty seven boxes of whole sections were preserved by freezing for shipment to Ocean Drilling for further geochemical studies. Some X-radiographs were made.

DOWN HOLE TOOLS

The new Barnes porewater and pressure sampler was deployed 23 times before it was lost due to a rare mechanical failure in the core barrel that allowed the tool and its pressure barrel to fall out of the bit. This could happen because the instrument is allowed to freefall down the string, with the bit off the bottom of the hole, and to penetrate the sediment. This decoupling of the core barrel permits formation pressure readings that do not reflect bit weight on the bottom of the hole or ship surge that may be transmitted down the string. Fishing for the tool was unsuccessful. In the 22 successful runs, battery failure was a recurrent problem. Water collected by the tool was analyzed, revealing unexpected water chemistry trends with ion concentrations far beyond expected ranges. Sediments characteristic of the deeper parts of the holes were typically fractured, allowing bottom water to seep in with the pore water and making dilution corrections necessary. Indeed, pressure measurements were the motivation for the deeper runs, with water a bonus.

CHEMISTRY

The diverse interests and high core recovery created a work load that required a high degree of organization. The scientists participated with the technicians in this effort. Hydrocarbon analyses, required by the safety guidelines, were followed by chromatograms detailing the light gases and heavy components, associated with life/climate cycles. The inorganic chemistry of interstitial waters samples provided the highest values ever recorded in ocean sediments. Clathrate specimens were collected in pressure vessels to study gas volumes and composition. Special intricate samples were collected to give biochemists the best chance of locating biological activity.

Complementing the lab's productivity was the addition of a thermal printer, two detectors on the DIONEX ion analyser, and the CARLE gas chromatograph to the HP 1000 Lab Automation System (LAS). New menus and a switch box made communication with the VAX easier for users of the ROCKEVAL and CAHN. New plotting routines on the VAX made data plotting easier. The new HP 3393 integrator, purchased for the CARLE gas chromatograph, allowed multi-level calibration for non-linear standard curves for the first time. The results were impressive in accuracy and time saved.

XRD/XRF LAB

Approximately 250 samples were prepared and analyzed on the X-ray diffractometer. Some of this effort was to evaluate XRD methods for determining opal content of the samples. Another technician was trained in the use of the XRD.

The X-ray fluorescence unit was used to analyze some 30 samples, including standards. Sample preparation was altered to some extent to accommodate sediment samples instead of rocks, primarily by adjusting the weight of sample downward to conserve it.

THIN SECTION LAB

Work for the thin section lab was moderate; all equipment functioned well. Forty petrographic slides were made and polished; six of the billets required epoxy impregnation. Phosphate nodules were unusual materials to section. The DATATRIEVE data base was translated to the S1032 system used on other lab data bases.

SCANNING ELECTRON MICROSCOPE

Paleontologists requested over 250 micrographs taken with this unit, documenting forams magnified near 200X. The unit was trouble free.

COMPUTER SERVICES

Classes in CT*OS, SAM and PicSure were conducted in port, getting the newcomers familiar with the system and informing them of the services available. New software was introduced to calculate sub-bottom depths that are assigned to sample ID.

New plotters were deployed in three areas, allowing users to see their results locally. Several terminals are now on the Local Area Net (LAN) and can for the first time store and retrieve information with the VAX in real time. Other terminals have menus installed that eliminate keywork going between programs.

PHOTO LAB

The photographer, new to the staff, and photo lab were able to handle all the routine and special photo requests and had no problems with print volume or equipment.

ELECTRONICS LAB

Areas that required occasional attention were the downhole tools, MASSCOMP computers, XRF and XEROX machines. The ET split underway watches with the geophysical tech, and assisted with shooting off a stuck bottom hole assembly.

STOREKEEPER

A modest ship store was opened, initially offering t-shirts, sweatshirts and "Resolution" notecards. More items will be added.

SPECIAL PROJECTS

A current meter and deployment system was designed for the coming Antarctic legs to determine current speed and direction to aid predictions of iceberg movement and positioning the ship. The system includes a Neil Brown current meter that gives current speed and direction and is tilt-corrected. It also gives temperature and pressure information. An IBM PCXT located in the ship's dynamic-positioning office processes the data and graphs it via SAIL software. An InterOcean electric winch was mounted on the starboard side mezzanine adjacent to the taut-wire boom. The winch will be re-fitted with an air motor to comply with regulations pertaining to its operation near the moonpool. The ship's welders constructed an A-frame boom that is manipulated vertically by a Beebe air tugger. The current meter was deployed successfully on 23 November and was used on most sites for the remainder of the leg, except shallow sites when the taut wire was in use. Several refinements to the system, including making the data VAX compatible (for finer plotting capabilities) will be finished before Leg 113.

SAFETY

Two-hour "bubble watches" for the techs were maintained at each of the shallow sites to assure that no gas problems interfered with operations.

A stuck drill pipe in Hole 682A made it necessary to sever the drill pipe with an explosive charge. It was the first time this Sedco crew has had to utilize this special training. Using the books and notes the job was done. An explosives handling checklist was written for the METS notebook in the Technician office.